

Article

Morphological and Structural Responses of *Albizia lebeck* to Different Lead and Nickel Stress Levels

Mahak Naveed¹, Maria Ghaffar^{2,3}, Zafran Khan¹, Nimra Gul¹, Iram Ijaz⁴, Amir Bibi¹, Soha Pervaiz^{5,†}, Hesham F. Alharby⁶, Muhammad Sayyam Tariq⁵, Syed Riaz Ahmed^{1,5,†}, Khalid Rehman Hakeem^{6,*} and Daniel K. Y. Tan^{7,*}

- ¹ Department of Plant Breeding and Genetics, Faculty of Agriculture Sciences, University of Agriculture Faisalabad, Faisalabad 38000, Pakistan; mahaknaveed@gmail.com (M.N.); zafrankhan.mandokhail@gmail.com (Z.K.); nimratahir12@yahoo.com (N.G.); ameerbibi@uaf.edu.pk (A.B.); syedriaz1920@gmail.com (S.R.A.)
- ² Nuclear Institute for Agriculture and Biology, Faisalabad 38850, Pakistan; kmona9850@gmail.com
- ³ Department of Plant Sciences, Quaid-i-Azam University, Islamabad 45320, Pakistan
- ⁴ Laboratory of Molecular Systematics and Evolution Genetics, Florida Museum of Natural History, University of Florida, Gainesville, FL 32611, USA; iramijaz643@gmail.com
- ⁵ Nuclear Institute for Agriculture and Biology, Pakistan Institute of Engineering and Applied Sciences (PIEAS), Islamabad 45650, Pakistan; sohasaroya123@gmail.com (S.P.); sayyamtariq@gmail.com (M.S.T.)
- ⁶ Department of Biological Sciences, Faculty of Science, King Abdulaziz University, Jeddah 21589, Saudi Arabia; halharby@kau.edu.sa
- ⁷ Faculty of Science, Plant Breeding Institute, Sydney Institute of Agriculture, School of Life and Environmental Sciences, The University of Sydney, Sydney, NSW 2006, Australia
- * Correspondence: kur.hakeem@gmail.com or khakim@kau.edu.sa (K.R.H.); daniel.tan@sydney.edu.au (D.K.Y.T.)
- † These authors contributed equally to this work.



Citation: Naveed, M.; Ghaffar, M.; Khan, Z.; Gul, N.; Ijaz, I.; Bibi, A.; Pervaiz, S.; Alharby, H.F.; Tariq, M.S.; Ahmed, S.R.; et al. Morphological and Structural Responses of *Albizia lebeck* to Different Lead and Nickel Stress Levels. *Agriculture* **2023**, *13*, 1302. <https://doi.org/10.3390/agriculture13071302>

Academic Editors: Murtaza Khan and Sajid Ali

Received: 6 May 2023

Revised: 17 June 2023

Accepted: 20 June 2023

Published: 26 June 2023



Copyright: © 2023 by the authors. Licensee MDPI, Basel, Switzerland. This article is an open access article distributed under the terms and conditions of the Creative Commons Attribution (CC BY) license (<https://creativecommons.org/licenses/by/4.0/>).

Abstract: Lead (Pb) and nickel (Ni) are serious soil pollutants that adversely affect plant growth and development and need to be removed through phytoremediation. The present study aimed to assess the morphological indices of *Albizia lebeck* (L.) (Benth.) in relation to anatomical modifications for survival under both Pb and Ni stress. The seedlings of *A. lebeck* were established and then subjected to four different concentrations, viz. 0 mM, 25 mM, 50 mM and 75 mM, of Pb and Ni for 14 days in two phases. Morphological traits such as shoot length (70.93%), fresh weight (79.27%), dry weight (83.9%), number of root hairs (65.7%), number of leaves per plant (67.4%) and number of leaflets per plant greatly reduced under Pb or Ni stress. Surprisingly, root length increased rather than decreased with the increase in Pb or Ni concentrations, along with an increase in leaflet width, leaflet length and leaflet area. Moreover, root cortical cell area, metaxylem area and phloem area decreased at 75 mM of Pb and Ni while epidermal thickness and cell area increased. Stem epidermal thickness, cell area and phloem area significantly decreased with the consistent increase in metaxylem area and cortical region thickness under both Pb and Ni stress. Leaf anatomical traits such as midrib thickness, abaxial epidermal thickness and stomatal density and adaxial epidermal thickness and stomatal area significantly increased with increasing Pb or Ni stress. Correlation analysis revealed close relations among morphological and anatomical traits (such as root length with cortical region thickness) for better plant survival under Pb or Ni stress, and a PCA-biplot further verified these correlation analyses. Cluster analyses demonstrated the associations among the morphological and anatomical traits based on different stress levels. Furthermore, we found that the longer exposure (from phase 1 to phase 2) of heavy metals stress is more dangerous for plant survival and can ultimately lead to plant death. Moreover, our results also confirmed that Ni is more harmful or dangerous to plants than Pb at high and moderate concentrations. The anatomical modifications ensured the survival of *A. lebeck* in extreme heavy metals stress and therefore unlocked its potential to be used as a natural source of phytoremediation. We also recommend that the genetic potential of *A. lebeck* associated with its survival under heavy metal stress be investigated.

Keywords: *Albizia lebbbeck*; lead nitrate; nickel nitrate; structural modifications; phytoremediation

1. Introduction

Several United Nations Sustainable Development Goals (SDGs), such as climate change regulation, sustainable cities and ecosystems, well-being, and good health, face serious challenges from soil pollution (presence of heavy metals) [1,2]. Environmental stressors associated with soil pollution, either from anthropogenic or natural sources, are directly affecting ecosystems' functions and biodiversity [3] and further compromising ecosystems' resilience to natural disaster and climate change. Furthermore, soil pollution in urban areas could adversely affect human health via cross-media migration-induced risk, e.g., heavy metals in drinking water, accumulation in plant tissues and organic contaminants vapor intrusion [4,5]. Presently, soil pollution is associated with poor waste management, overuse of pesticides, weeds, industrial processes and vehicle emissions [6]. Soil contains a variety of heavy metals and their effects on plants can be beneficial or toxic depending on their concentration. Heavy metals such as cobalt (Co), nickel (Ni), copper (Cu) and zinc (Zn) are considered essential for plant growth but in low concentrations, because at high concentrations, they become toxic. Other heavy metals, such as mercury, lead (Pb), cadmium (Cd) and arsenic (As), are considered toxic even at low concentrations as they inhibit plant growth [7]. The presence of heavy metals in Pakistani soil is of great concern and has become a serious threat to the agriculture sector. Scarcity of surface water and depletion in groundwater levels has forced farmers to use wastewater as an alternative source of irrigation for crops in Pakistan [8]. Wastewater released from industries is composed of a large amount of heavy metals and its application to crops results in a high accumulation of heavy metals in Pakistani soil [9]. Therefore, the accumulation of these metals is increasing over time and affecting crop growth and development. The concentration (minimum to maximum) of heavy metals present in the soil varies from area to area and city to city in Pakistan [10]. The areas/cities near industries (including Faisalabad, Lahore, etc.) contain large amounts of heavy metals and adversely affect arable lands. Several studies have been conducted to report the effect of heavy metals on plant growth and development. Lead and nickel are the most widespread heavy metals that come from various human activities [11,12]. Once Pb or Ni is bound intracellularly or on the cell surface, they interact with polysaccharides, nucleic acids and proteins and thereby cause metabolic disorders, as well as stunted plant growth [13,14].

Since Pb is an inorganic, non-biodegradable pollutant and toxic element, its long-term tenacity in soil poses a major threat to the environment. Just like the concentration of other heavy metals, the accumulation of Pb in soils of Pakistan is also increasing over time. The concentration of Pb always differs from soil to soil and region to region. Therefore, different studies across Pakistan have been conducted to assess the concentration of Pb in the soil of different regions. For example, in the soils of Dera Ghazi Khan (Punjab, Pakistan), the Pb concentration ranged from 0.01–1.17 mg kg⁻¹ (after wastewater application it increased to 0.13–2.08 mg kg⁻¹) [12,15], in Kasur (Punjab, Pakistan) from 2.12–3.12 mg kg⁻¹ [16], in Faisalabad (Punjab, Pakistan) from 7.54–41.45 mg kg⁻¹ [17], in Khyber Pakhtunkhwa (KPK, Pakistan) from 0.02–23.02 mg kg⁻¹ [18], and in Islamabad (Pakistan) from 40–90 and 60–150 mg kg⁻¹ [19]. Excess Pb in soil induces alterations in plant morphological and anatomical structures, as well as physiological and biochemical processes, resulting in chlorosis, growth retardation, low biomass and seed yield [20]. Removing Pb from the soil is challenging due to its low bioavailability, as it forms strong bonds with inorganic and organic soil ligands. Due to the low mobility of Pb in the soil, Pb tolerant plants may sometimes concentrate Pb in their roots with little ability to transfer it to aboveground parts [21]. In this context, testing metal-tolerant plant species to determine whether they are able to accumulate Pb from soil in their roots or translocate it to shoots becomes extremely important. Ni is essential for plant growth and

development and is associated with many critical roles in plants but become toxic at high concentration. Ni is also known as an environmental pollutant present in both liquid and solid forms and accumulates in soil from industrial and municipal discharged waste [22]. Excess Ni induces stress and alters metabolic processes, causing mineral imbalance, reduction in respiration and photosynthesis rate, production of reactive oxygen species (ROS) and oxidative damage by disturbing the antioxidant defensive systems of plants [23]. The concentration of Ni also varies in soil across Pakistan. For example, in Dera Ghazi Khan, Ni concentration ranged from 0.02–0.19 mg kg⁻¹ (after wastewater application 0.87–7.87 mg kg⁻¹) [15], in Faisalabad (1.53–6.87 mg kg⁻¹) [17], in Islamabad (41.4–59.3 mg kg⁻¹) [24], in Vehari (0.7–3.5 mg kg⁻¹) [25], in Khyber Pakhtunkhwa (KPK, 0.02–18.98 mg kg⁻¹) [18,26] and in Abbottabad (8.07–8.50 mg kg⁻¹) [27]. Basic igneous rocks and argillaceous sediments contain around 500 mg kg⁻¹ of Ni and serpentine soils can contain several thousand mg kg⁻¹ Ni [28,29].

Plants, being sessile organisms, are permanently confined to their germination site and are thus consistently challenged by several abiotic stresses including heavy metals. To reproduce and survive in an ever-changing environment, plants need to balance their growth and environmental responses [30]. To compensate for their lack of mobility, plants have developed unique mechanisms enabling them to quickly react to changing environmental conditions and flexibly adapt their post-embryonic developmental program [31]. Plants grown in contaminated root media provide a model for studying mechanisms of metal accumulation and tolerance. Plant adaptation to changing environments varies from one plant species to others. To cope with heavy metals stress, plants adopt several structural (anatomical and morphological) and functional responses. Moreover, plants have also evolved various structural modifications such as increased epidermal thickness, decreased stomatal density and stomatal area, metaxylem area and bulliform cells to overcome heavy metals stress [32–34]. The accumulation of Pb and Ni in root, leaf and stem tissues modifies anatomical structures and make plants more susceptible to heavy metals stress [35–40]. These processes mostly take place at the tissue level and vary from plant to plant, and even in the populations of a single species, due to differences in microclimate [41]. Exploring these inherited adaptive potentials of plant species can be helpful in augmenting the scientific community's efforts towards the development of heavy metal resistant plant species.

A. lebbeck, locally called Siris, is a highly important agroforestry tree species cultivated in arid and semi-arid regions of Pakistan and other parts of the world like West and South African countries. It has the ability to accumulate a large amount of heavy metals [42], and is therefore considered as an excellent source of phytoremediation, adapted to wide range of environmental conditions [43]. However, the effect of heavy metals on the cellular structure and function features of *A. lebbeck* is still unknown. When plants are exposed to prolonged heavy metal stress, several structural and functional changes occur at the cellular level. It was hypothesized that *A. lebbeck* may respond differently to Pb or Ni stress by adopting structural modifications. To date, very limited studies have been conducted on the effects of heavy metals on *A. lebbeck*. Furthermore, to the best of our knowledge, the effect of both Pb and Ni on anatomical modifications has not yet been explored in the species *A. lebbeck*. So, keeping in view the variation in concentration of Pb and Ni across soils in Pakistan and worldwide, it is therefore important to explore the response of *A. lebbeck* to different levels of Pb or Ni stress. The present study therefore aimed to assess the morphological indicators of *A. lebbeck* in relation to anatomical modifications for survival under both Pb and Ni stress.

2. Materials and Methods

2.1. Plant Material and Growth Conditions

The present study was conducted in the research area of the Department of Botany, University of Agriculture, Faisalabad, Pakistan. Certified seeds (disease free) of *A. lebbeck* were purchased from a government certified supplier of the local market of Pattoki, Punjab, Pakistan. Before sowing, sodium hypochlorite [10% (v/v)] was used to sterilize seeds for

10 min to ensure maximum germination. After sterilization, the seeds were soaked in distilled water overnight. After soaking, the healthy seeds (seeds with uniform sizes) were kept in glass Petri dishes (150 mm Ronyes Lifescience) lined with Whatman™ (cytiva; grade 40) filter papers dampened with Hoagland solution (half strength) at pH 6.5. Petri-dish were kept in the dark for germination at 28 ± 2 °C for 4 days and were grown under a PPFD (photosynthetic photon flux density) of $150 \mu\text{mol photon m}^{-2} \text{s}^{-1}$, a relative humidity (RH) of 55–65% with a 16/8 h light/dark cycle at 28 ± 2 °C for 10 days in a growth chamber (PGI-550VH). Seedlings with uniform sizes were selected and then transferred into pots (12 cm W and 10 cm L). All pots were uniformly filled with soil containing 60% sandy soil and 40% loamy soil (containing organic matter (0.74%), nitrogen (0.73%), phosphorus (8.1 mg kg^{-1}), potassium (169 mg kg^{-1}), with electrical conductivity ($\text{EC } 2.84 \text{ dS.m}^{-1}$) and pH (7.60)) with three replications (R1, R2 and R3) using a complete randomized design (CRD). A total of ten seedlings were transferred into each pot. Two days after seedling transformation, lead nitrate [$\text{Pb}(\text{NO}_3)_2$] and nickel nitrate [$\text{Ni}(\text{NO}_3)_2$] treatments of varying concentrations such as 0 mM (as control), 25 mM, 50 mM and 75 mM were given to seedlings continuously for 14 days in two phases [i.e., phase 1 (stress for only 7 day) and phase 2 (stress for 14 days)] (Figure 1). After 7 days of heavy metal stress, five seedlings from each pot in each replication were harvested randomly and were subjected to recording of morphological data only. In phase 2, the heavy metal stress was continued for the next 7 days (that is, from the 8th to 14th day) for the remaining five seedlings. After that, the remaining seedlings were harvested, and morphological and anatomical data were recorded. For studying anatomical parameters, the seedlings were fixed for 72 h in formalin acetic alcohol (FAA) prepared by mixing 35% distilled water, 50% ethyl alcohol, 5% acetic acid and 10% formalin *v/v* [44], and then transferred to acetic acid solution for long term storage. $\text{Pb}(\text{NO}_3)_2$ (Sigma Aldrich) containing Pb and $\text{Ni}(\text{NO}_3)_2 \cdot 6\text{H}_2\text{O}$ (nickel nitrate hexahydrate) containing Ni were used to prepare metal-solutions of different concentrations. These concentrations are based on the outcomes of comprehensive screening experiments and are also environmentally relevant [28,45–51].

2.2. Measurements of Morphological Parameters

Morphological parameters such as shoot length (cm), root length (cm), number of root hairs, number of leaves per plant, leaflet length (cm), leaflet width (cm), leaflet area (cm^2), number of leaflets per leaf, leaf area (cm^2), and fresh and dry weight (g plant^{-1}) were measured after harvesting the control and differentially Pb- and Ni-treated *A. lebbek* seedlings in both phase 1 (after 7 days of treatments) and phase 2 (after 14 days of treatments). After harvesting, distilled water was used to wash seedlings, shoots and roots carefully to completely remove any soil. The seedlings were then carefully placed on paper towel to remove the water crystals and their fresh weights were recorded. Fresh weight (g plant^{-1}) was measured using an electronic analytical weighing balance. To record dry weight (g plant^{-1}), each seedling was placed in butter-paper and oven dried at 65 ± 2 °C until a constant weight was obtained.

2.3. Anatomical Study

After recording the morphological parameters, the seedlings preserved in FAA were used to study anatomical variations in *A. lebbek* caused by Pb or Ni stress. Different anatomical parameters were recorded in the root, stem and leaf. A total of three anatomical sections were made from each plant organ (root, stem and leaf). A 2 cm piece of the thickest root (immediately after cutting the root cap), a 2 cm piece of stem (uppermost part) and a 2 cm piece of a leaf from the leaf base were taken for sectioning. All tissue and cell measurements were taken using an ocular micrometer which was calibrated with a stage micrometer.

2.3.1. Root Anatomy

Preserved root samples of control and differentially Pb- and Ni-treated *A. lebbek* seedlings were taken and a transverse section was cut using the freehand technique. The

sections were then transferred onto clean slides containing a drop of water, and 50% safranin was used to stain samples, which were then mounted on glycerin. The specimens were covered with a cover-slip and images were taken through a digital camera linked with light-microscope (Nikon 104, Japan). Different internal structures of the root such as epidermal thickness [RETh (μm)], epidermal cell area [RECA (μm^2)], cortical region thickness [RCrTh (μm)], cortical cell area [RCrCA (μm^2)], metaxylem area [RMA (μm^2)] and phloem area [RPhA (μm^2)] were observed.

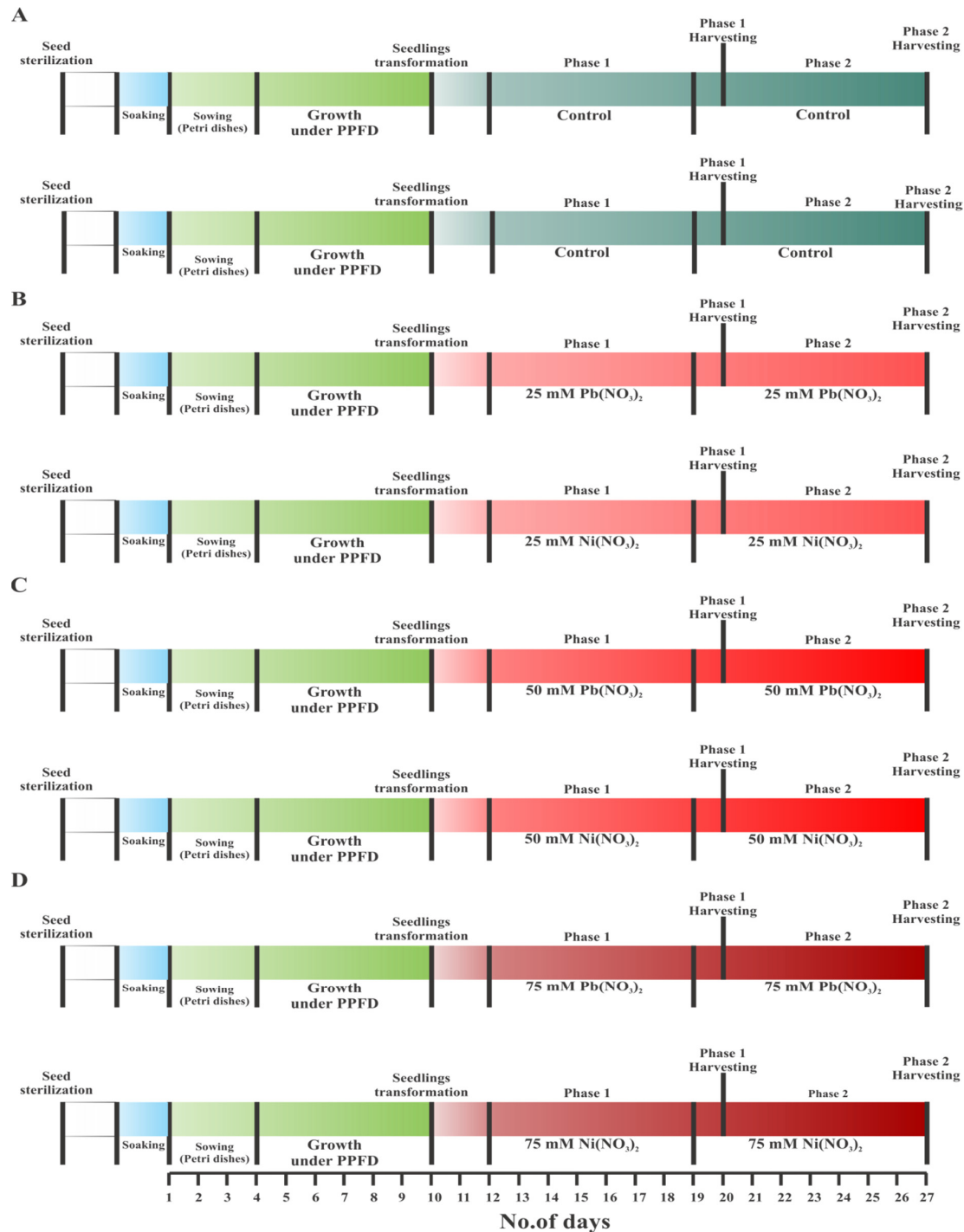


Figure 1. Graphical representation of methodology and treatments followed to conduct the current study for better understanding. (A) control conditions (without Pb and Ni stress), (B) stress conditions at 25 mM of Pb and Ni, (C) stress conditions at 50 mM Pb and Ni, and (D) stress conditions at 75 mM of Pb and Ni.

2.3.2. Stem Anatomy

Preserved stem samples of control and differentially Pb- and Ni-treated *A. lebbeck* seedlings were taken and a transverse section was cut using the freehand technique, similar to that for root anatomy. The sections were then transferred onto clean slides containing a drop of water, and 50% safranin was used to stain samples, which were then mounted on glycerin. The specimens were covered with a cover-slip and images were taken through a digital camera. Different internal structures of the stem such as epidermal thickness [SETh (μm)], cell area [SECA (μm^2)], cortical region thickness [SCrTh (μm)], cortical cell area [SCrCA (μm^2)], metaxylem area [SMA (μm^2)], and phloem area [SPhA (μm^2)] were observed.

2.3.3. Leaf Anatomy

Preserved leaf samples of the control and differentially Pb- and Ni-treated *A. lebbeck* seedlings were taken and a transverse section was cut using the freehand technique, similar to that for root and stem anatomy. The sections were then transferred onto clean slides containing a drop of water, and 50% safranin was used to stain samples, which were then mounted on glycerin. The specimens were covered with a cover-slip and images were taken through a digital camera. Different internal structures of the leaf such as midrib thickness [LMdTh (μm)], lamina thickness [LLmTh (μm)], adaxial epidermal thickness [LADET (μm)], adaxial epidermal cell area [LADECA (μm^2)], abaxial epidermal thickness [ABET (μm)], abaxial epidermal cell area [LABECA (μm^2)], adaxial stomatal density [LADSD (mm^{-2})], adaxial stomatal area [LADSA (μm^2)], abaxial stomatal density [LABSD (mm^{-2})] and abaxial stomatal area [LABSA (μm^2)] were observed.

2.4. Statistical Analyses

All the morphological and anatomical traits data was subjected to three-way and two-way factorial analysis of variance (ANOVA) ($p < 0.05$ & 0.001), respectively. Pairwise-mean comparison was performed through Tukey's honestly significant difference (HSD) test ($p < 0.05$). Moreover, Pearson's correlation coefficient analyses were performed to measure the correlation between all the morphology traits recorded and the anatomy traits of root, stem and leaf, separately. Multivariate analysis: principal components analysis (PCA) biplots and cluster-heatmaps were constructed to reduce the dimensionality of the data and to observe the pattern of association in traits under different concentrations of metals, respectively. Data manipulation and analyses were performed in RStudio (Version 4.2.2) using packages agricolae, stats, corrplot, pheatmap, Factoextra, FactoMineR, GGally, ggplot2 and metan.

3. Results

Analysis of variance (ANOVA) revealed that all the main effects (time, metals, and concentrations) investigated exhibited extremely significant variations for all the morphological features. The two- and three-way interactions were also highly significant for all the traits, except shoot length and fresh weight, where concentration \times metal interaction was non-significant. These findings suggest that the morphology of *A. lebbeck* is influenced by the duration of the stress, its concentration and the type of metal used (Supplementary Table S1).

Concentration level had a substantial impact on all the examined anatomical features, except LADSD. The majority of the root and leaf anatomical attributes were significantly influenced by the source of metal; however, only the SCRT demonstrated a significant change in the stem anatomical traits. The interaction effect (concentration \times metal) showed significant effects on anatomical traits like SECA, SCRT, RETH, REpCA, RphlA, LMdTh, LLmTh, LABECA, LADECA and LABSA, while the rest of the root, stem and leaf traits showed non-significant differences (Supplementary Table S2). These findings suggest that the concentration of the metal is the primary variable influencing the internal structure of the plant tissue.

3.1. Lead and Nickel Both Reduced Seedling Growth and Enhanced Root Length

A. lebbek seedlings were exposed to Pb or Ni stress at two time periods (i.e., Phase 1 and Phase 2) to evaluate the effect on shoot and root traits. After 14 days of heavy metal stress, the symptoms were evident, including chlorotic circle spots on leaves and dryness of leaves edges. Shoot length decreased significantly ($p < 0.05$) with increasing concentrations of Pb and Ni in both time periods. The maximum reduction in shoot length was recorded as 70.93% (at 75 mM Ni stress in phase 1) and 48.87% (at 25 mM Pb stress in phase 2) compared to the control (Figure 2A). On the other hand, root length increased with increasing concentrations of Pb and Ni in both phases (except for 75 mM Pb and 75 mM Ni in phase 1 and 2, respectively). The maximum increase in root length was recorded as 48.94% (at 25 mM Ni in phase 1) and 55.71% (at 75 mM Pb in phase 2) compared to the control (Figure 2B). Pb or Ni stress also adversely affected fresh and dry weights (g Plant^{-1}) in all seedlings of *A. lebbek*. Both fresh and dry weights were significantly ($p < 0.05$) reduced with increasing concentrations of Pb and Ni in both phases. The maximum reduction in fresh weight was recorded as 50% (at 50 mM Ni in phase 1) and 79.27% (at 75 mM Ni in phase 2) (Figure 2C). A similar trend was observed for dry weight, where the maximum reduction was recorded as 77.3% (at 50 mM Ni in phase 1) and 83.9% (at 75 mM Ni in phase 2) (Figure 2D). Overall, nickel nitrate showed more drastic effects on fresh and dry weight than lead nitrate.

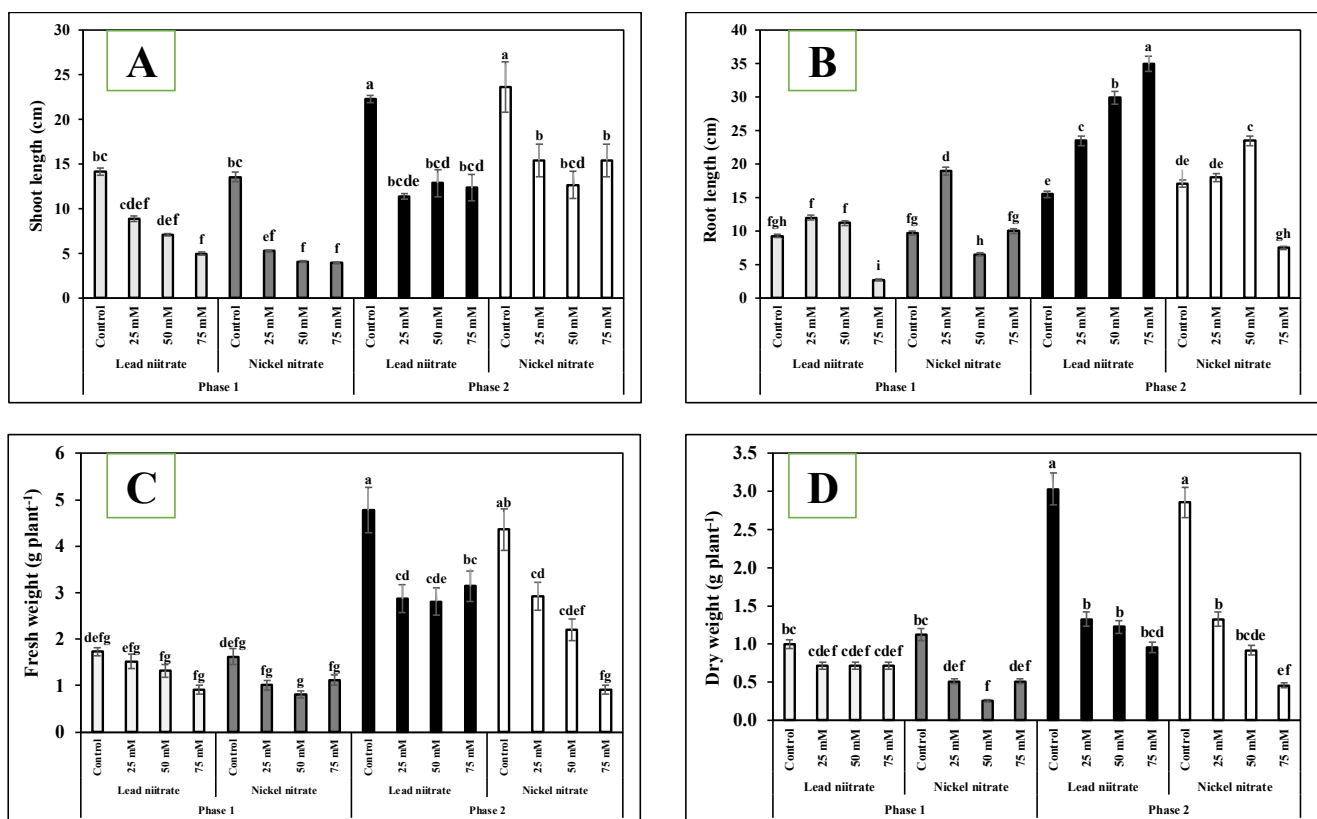


Figure 2. Effect of different Pb and Ni concentration levels on (A) shoot length (cm), (B) root length (cm), (C) fresh weight (g plant^{-1}) and (D) dry weight (g plant^{-1}) in two phases. The means with the same letters are not significantly different at $p < 0.05$.

3.2. Effect of Lead and Nickel on Number of Root Hairs and Leaf Morphology

As shown in Figure 3A,B, the significant differential growth between control and treatments can be clearly observed. The number of root hairs and number of leaves per plant reduced significantly ($p < 0.05$) with the increase in Pb and Ni concentrations in both time periods. For example, the highest reduction in number of root hairs was recorded

as 65.7% (at 75 mM Pb in phase 1) and 51.5% (at 75 mM Ni in phase 2) compared to the control (Figure 3A). Furthermore, at 25 mM of Pb (in phase 2) the number of root hairs increased rather than decreased compared to control (Figure 3A). The effects of both Pb and Ni were also phenotypically characterized by a significant ($p < 0.05$) reduction in the number of leaves per plant. Similarly, the maximum reduction in number of leaves per plant was recorded as 67.4% (at 75 mM Ni in phase 1) and 66.5% (at 75 mM Ni in phase 2) compared to the control (Figure 3B).

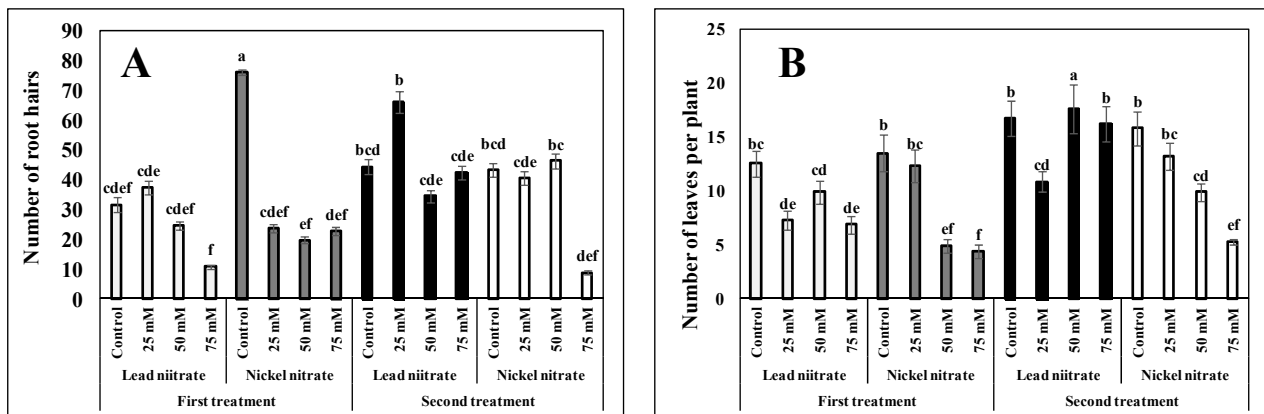


Figure 3. Effect of different Pb and Ni concentration levels on (A) number of root hairs, and (B) number of leaves per plant in two phases. The means with the same letters are not significantly different at $p < 0.05$.

Pb or Ni treatments induced a significant ($p < 0.05$) increase in leaflet length and leaflet width, resulting in increased leaflet area (cm^2) in both phases. The highest increase in leaflet length was recorded as 43.7% and 31.6% at 50 mM Ni in both phase 1 and phase 2, respectively, compared to the control (Figure 4A). Similarly, the leaflet width increased by 67.3% and 7.0% at 25 mM of Ni stress in phase 1 and phase 2, respectively, compared to the control (Figure 4B). The increase in leaflet length and width enhanced leaflet area (cm^2) by 68.5% (at 75 mM Pb in phase 1) and 63.1% (at 50 mM Pb in phase 2) compared to the control (Figure 4C). However, at 50 and 75 mM of Ni stress in phase 1 and phase 2, leaflet area reduced rather than increased. Furthermore, the number of leaflets per leaf slightly reduced under all treatments (except for 75 mM of Ni in phase 1) compared to the control (Figure 5A). Nickel nitrate showed more severe effects on leaf area than lead nitrate and reduced it dramatically at 75 mM of concentration (95.2% and 54.5% in phase 1 and phase 2, respectively) (Figure 5B). Notably, lead nitrate promoted the leaf area in both phases.

3.3. Effects of Lead and Nickel Nitrate on Anatomical parameters

3.3.1. Root Anatomy

RCrCA (μm^2), RMA (μm^2) and RPhA (μm^2) decreased consistently with increasing Pb and Ni concentrations (Table 1, Figure 6B,C). RCrCA, RMA and RPhA decreased by 47.8%, 60.5% and 55.9% at 75 mM Pb and 57.7%, 64.2% and 62.1% at 75 mM Ni, respectively, compared to the control. RCrTh (μm) increased consistently with increasing Pb and Ni concentrations. RCrTh increased by 105.9% and 132.5% at 75 mM Pb and Ni, respectively. RETH (μm) increased by 226.6% and 186.4% at 25 and 50 mM Pb, respectively, while at 75 mM Pb, it increased by only 53.3%. Similarly, under Ni stress, RETH increased by 64.8% and 53.7% at 75 mM and 25 mM, respectively, but only by 20.5% at 50 mM. RECA (μm^2) under lead and nickel nitrate stress showed the maximum expansion at 25 mM and 50 mM, respectively (Table 1).

3.3.2. Stem Anatomy

SETh (μm), SECA (μm^2) and SPhA (μm^2) significantly decreased with increasing Pb and Ni concentrations. SETh, SECA and SPhA decreased by 66.4%, 68.7% and 42.4%

at 75 mM Pb and 67.7%, 69% and 52.8% at 75 mM Ni, respectively, in comparison with the control (Table 1). SCrCA (μm^2) increased by 37.6% and 0.1% at 25 mM of Pb and Ni, respectively, but decreased by 21% (at 50 mM Pb), 49.3% (at 75 mM Pb), 57.6% (at 50 mM Ni) and 65.3% (at 75 mM Ni) (Figure 6D,E). SMA continuously increased with increasing Pb and Ni concentrations. SMA increased by 77% and 168.2% at 75 mM of Pb and Ni, respectively. SCrTh increased under both stresses with increasing stress level, while it decreased by 37.4% under Pb stress only at 25 mM.

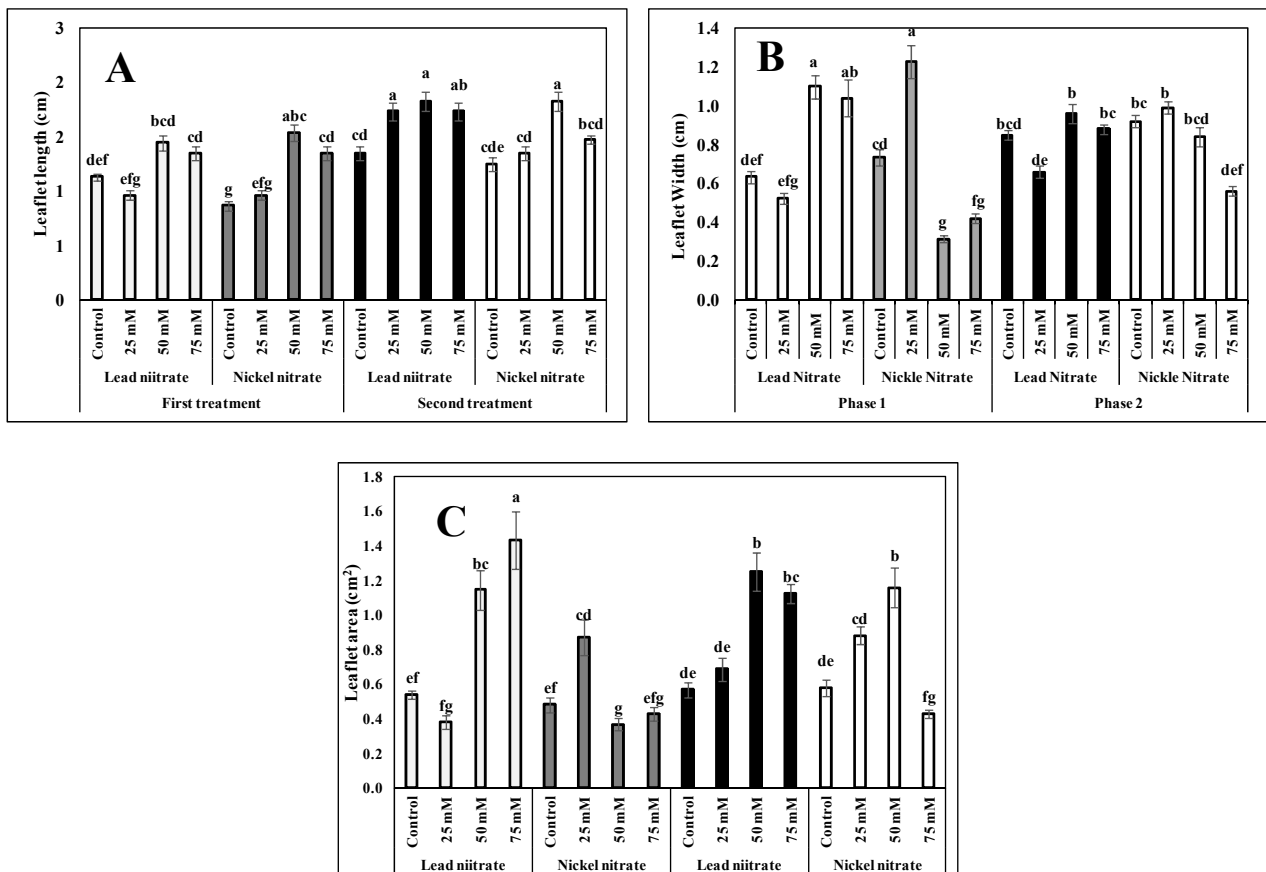


Figure 4. Effect of different Pb and Ni concentration levels on (A) leaflet length (cm), (B) leaflet width (cm) and (C) leaflet area (cm^2) in two phases. The means with the same letters are not significantly different at $p < 0.05$.

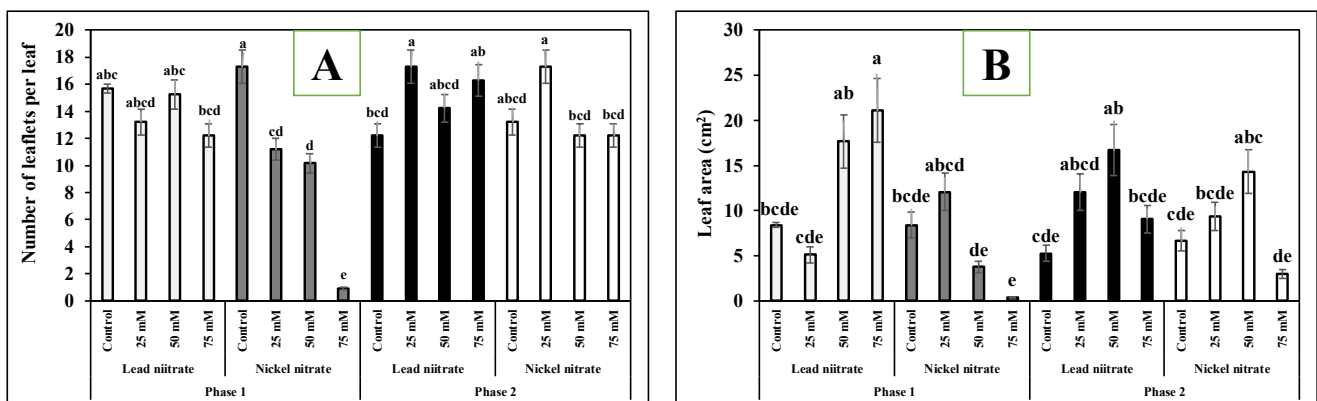


Figure 5. Effect of different Pb and Ni concentration levels on (A) number of leaflets per leaf, and (B) leaflet area (cm^2) in two phases. The means with the same letters are not significantly different at $p < 0.05$.

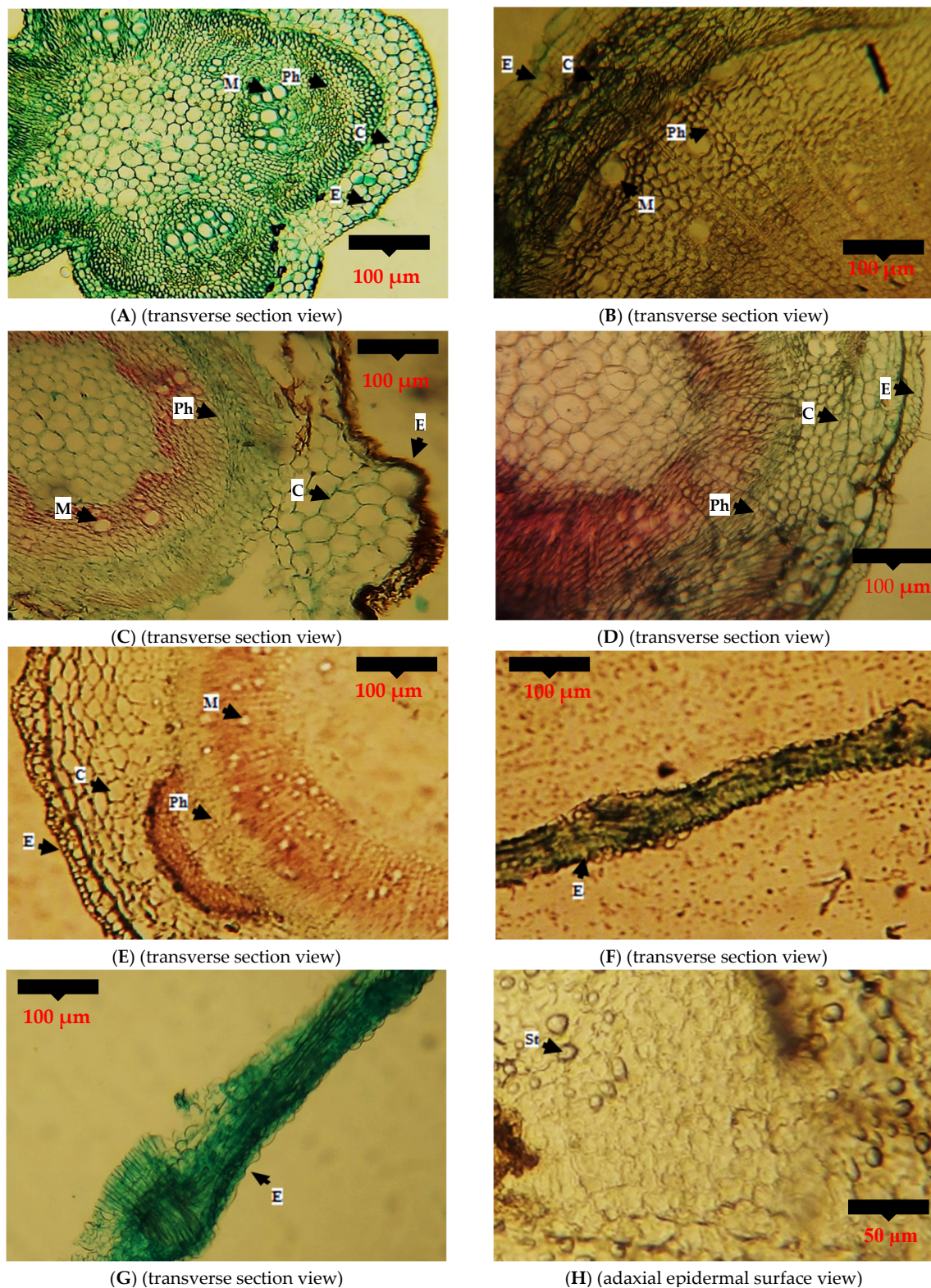


Figure 6. Effect of different levels of Pb or Ni stress on anatomical structures of *albizia lebeck*. (A) Root anatomical structure under 0 mM, (B) root anatomical structure under 50 mM Pb, (C) root anatomical structure under 75 mM Ni, (D) stem anatomical structure under 75 mM Ni (E) stem anatomical structure under 75 mM Pb, (F) leaf anatomical structure under 75 mM Pb, (G) leaf anatomical structure under 50 mM Ni and (H) leaf adaxial anatomical structure under 75 mM Ni. Abbreviations; M (metaxylem), Ph (phloem), C (cortical), E (epidermal) and St (stomata).

3.3.3. Leaf Anatomy

LMdTh (μm) of *A. lebbbeck* decreased with the increase in heavy metals concentration (Table 2), while it increased by 13.1% and 12.5% at 25 mM Pb and 50 mM Ni, respectively. LLmTh (μm) increased under both lead nitrate (at 25 and 50 mM) and nickel nitrate (at 50 mM and 75 mM) stress, but it also decreased by 3.1% and 70.2% at 75 mM Pb and 25 mM Ni, respectively (Table 2). LABET (μm) decreased with increasing Pb and Ni concentrations. The maximum reduction in LABET was recorded as 24.8% and 33.1% at 75 mM of Pb and Ni, respectively. Similarly, LADET (μm) also decreased with increasing Pb and Ni concentrations but increased by 11.8% at 25 mM Pb. LABECA (μm^2) reduced with increasing heavy metals concentrations, i.e., 25 mM and 50 mM, but slightly increased at 75 mM of Pb and Ni, compared to at 25 and 50 mM (Figure 6F,G).

LABSD (mm^{-2}) and LADSA (μm^2) decreased with increasing concentrations of Pb and Ni. LABSD and LADSA decreased by 54.1% and 59.3% at 75 mM of Pb and Ni, respectively. LABSA (μm^2) and LADSD (mm^{-2}) responded differently under both heavy metals (Table 2). LABSA decreased at 50 mM and 75 mM of Pb and Ni but increased by 25.3% and 132% at 25 mM of Pb and Ni, respectively. LADSD decreased under lead nitrate but increased under nickel nitrate (Figure 6H, Supplementary Figure S1). The maximum reduction was recorded at 50 mM (21.3%) and the maximum increase at 25 mM (22%).

3.4. Principal Component Analysis

Principal component analysis (PCA) was used to construct biplots between root anatomical and morphological traits, stem anatomical and morphological traits and leaf anatomical and morphological traits separately for Pb and Ni. The results for root anatomical and morphological traits (under Pb stress) showed that 81.6% of the total variance could be explained with the first two components (60.5% for PC1 and 21.1% for PC2). PC1 was characterized mainly by morphological traits such as root length, shoot length, fresh weight and dry weight. At the same time, PC2 was represented by epidermal thickness, epidermal cell area, cortical cell area, metaxylem area, phloem area, leaf area, leaflet length, leaflet width, leaflet area and number of leaves per plant. Root anatomical and morphological PCA biplot showed four isolated clusters (Figure 7A). The first cluster showed a strong association among morphological and anatomical traits like leaflet width, leaflet length, leaflet area, leaf area, number of leaflets per leaf, epidermal thickness and epidermal cell area at 25 mM Pb (C2). In the second cluster, morphological traits like root length and number of leaves per plant showed a weak association with cortical region thickness at 50 and 75 mM Pb (C3 and C4). The number of root hairs in the third cluster showed a weak correlation with phloem area, metaxylem area and cortical cell area. The fourth cluster showed strong associations among morphological traits like shoot length and fresh weight, while a weak association with dry weight. Similarly, the results for root anatomical and morphological traits under Ni stress showed a total of 90.6% variance (54.3% for PC1 and 36.5% for PC2) (Figure 7B). The PCA biplot showed three isolated groups, where the first cluster showed a strong association among morphological traits like leaflet width, leaflet length, leaflet area, leaf area, root length and number of root hairs, while a weak association with number of leaves per plant at 25 mM Ni (C2). Number of leaflets per plant, fresh weight, dry weight, shoot length, metaxylem area, phloem area and cortical cell area showed a strong association among each other in the second cluster at 0 mM Ni (C1). The third cluster showed a weak association among cortical thickness and epidermal thickness at 75 mM Ni (C4).

Table 1. Effect of Pb and Ni on root and stem anatomical traits of *Albizia lebbek* under different concentration levels.

Root Anatomy	Lead Nitrate				Nickel Nitrate			
	0 mM	25 mM	50 mM	75 mM	0 mM	25 mM	50 mM	75 mM
RETh	25.1 ± 2.1 b	82 ± 8.6 a	71.9 ± 7.5 a	38.5 ± 3.9 b	25.3 ± 4.2 b	38.9 ± 9.6 b	30.5 ± 10.4 b	41.7 ± 8.3 b
RECA	151.7 ± 13.8 d	1357.1 ± 398.1 a	1317 ± 42.9 a	475.4 ± 41.3 cd	147.3 ± 31.2 d	761.6 ± 50.5 bc	1053.5 ± 63.5 ab	642.5 ± 48.6 bc
RCrTh	124.9 ± 8 f	146.1 ± 10.1 ef	203.6 ± 15.8 cd	257.2 ± 22 ab	128.3 ± 5.6 f	168.9 ± 16.8 de	219.4 ± 17.2 bc	289.3 ± 2.2 a
RCrCA	969.8 ± 116.7 a	724.6 ± 41 bc	627 ± 12.9 cd	506 ± 83.5 cd	924.5 ± 147.3 ab	594.8 ± 70.7 cd	426.5 ± 39 d	390.2 ± 74.3 d
RMA	1824.9 ± 404.5 a	1327 ± 282.4 ab	1011.2 ± 36.5 bc	720.6 ± 61.7 c	1708.7 ± 287.3 a	1061.8 ± 69.1 bc	779.8 ± 39.1 bc	611.6 ± 43.4 c
RPhA	392.9 ± 42.2 a	333.2 ± 67.9 ab	248.7 ± 30.3 bc	173 ± 27.3 c	430.2 ± 42.9 a	230.6 ± 30.2	195.7 ± 28.5 c	162.7 ± 36.6 c
Stem Anatomy								
SETh	37.9 ± 4.8 a	25.3 ± 4.2 c	23.8 ± 1.8 c	12.7 ± 1.8 d	35.4 ± 3 ab	27 ± 2 bc	18.9 ± 2.1 cd	11.4 ± 3.3 d
SECA	482.6 ± 47.9 a	204.3 ± 12.7 bc	239.2 ± 27.1 b	150.6 ± 29.1 c	435.7 ± 39.4 a	264 ± 32 b	188.2 ± 21.5 bc	135 ± 14 c
SCrTh	117.7 ± 8.5 cd	143 ± 22.2 bc	73.6 ± 6.3 d	168.5 ± 26.5 bc	120.5 ± 11 cd	173.1 ± 12.5 b	155.8 ± 26.9 bc	225.8 ± 18.9 a
SCrCA	492.8 ± 39.4 ab	678.5 ± 114.5 a	389.2 ± 45.4 bc	249.6 ± 25.2 bc	659.6 ± 142.5 a	660.3 ± 142.2 a	279.2 ± 40.9 bc	228.6 ± 19.9 c
SMA	290.6 ± 15.2 e	920.3 ± 41.8 ab	690.4 ± 61.7 cd	514.6 ± 60.7 d	260.9 ± 39 e	942 ± 144.1 a	719.1 ± 40 bc	699.8 ± 89.1 cd
SPhA	368.6 ± 22.6 a	295.1 ± 36.5 abc	265.9 ± 20.1 bcd	212.3 ± 19.8 cd	375.3 ± 27.7 a	306.6 ± 65.8 av	245.2 ± 29 bcd	176.8 ± 9.5 d

Note: Means sharing same letter with regions are non-significant at $p \leq 0.05$. Abbreviations; RETh (epidermal thickness), RECA (epidermal cell area), RCrTh (cortical region thickness), RCrCA (cortical cell area), RMA (metaxylem area), RPhA (phloem area), SETh (epidermal thickness), SECA (epidermal cell area), SCrTh (cortical region thickness), SCrCA (cortical cell area), SMA (metaxylem area) and SPhA (phloem area).

Table 2. Effect of Pb and Ni on leaf anatomical traits of *Albizia lebbek* under different concentration levels.

Leaf Anatomy	Lead Nitrate				Nickel Nitrate			
	0 mM	25 mM	50 mM	75 mM	0 mM	25 mM	50 mM	75 mM
LMdTh (µm)	265.4 ± 12.7 b	300.2 ± 11 a	221 ± 16.6 d	165.4 ± 10.4 e	233.5 ± 4.1 cd	69.5 ± 8.6 f	262.7 ± 11 bc	172.3 ± 6.3 e
LLmTh (µm)	130.6 ± 6.3 bc	162.6 ± 15	166.8 ± 16.6 a	126.5 ± 13.3 c	119.5 ± 7.8 c	63.9 ± 8.6 d	140.3 ± 12.7 abc	128.4 ± 5.8 c
LABET (µm)	24.9 ± 2.8 a	22.3 ± 2.4 ab	21.7 ± 2.6 ab	18.7 ± 2.2 ab	23.2 ± 2.1 ab	20.1 ± 3 ab	17.9 ± 4.9 ab	15.5 ± 2.6 b
LABECA (µm ²)	313.5 ± 15 a	232.6 ± 62.7 ab	220.1 ± 12.1 abc	267.1 ± 23.3 a	323.3 ± 47.9 a	116.2 ± 33.2 cd	83.8 ± 65.8 d	138.2 ± 24.9 bcd
LADET (µm)	27.8 ± 6.3 ab	31.1 ± 8.5 a	26.4 ± 1.2 ab	18 ± 6.3 ab	25 ± 3.6 ab	25 ± 5.8 ab	19.4 ± 2.4 ab	13.9 ± 2.4 b
LADECA (µm ²)	226.1 ± 20.5 b	100.1 ± 56.8 b	117.7 ± 13.4 b	163.8 ± 24.1 b	223.4 ± 6.4 b	300.5 ± 70.9 ab	462.4 ± 199.6 a	95.4 ± 13.6 b
LABSD (mm ⁻²)	48.6 ± 3.5 a	35.3 ± 2 b	32.2 ± 1.3 bc	22.3 ± 3.5 de	45 ± 2.6 a	28.6 ± 2	25.6 ± 3 cde	18.3 ± 2.5 e
LADSD (mm ⁻²)	33.3 ± 1.5 bcd	29.3 ± 3.5 cd	26.2 ± 6.8 d	30.3 ± 3.5 bcd	36.3 ± 1.5 abc	44.3 ± 3 a	37.6 ± 0.5 abc	39.6 ± 2.5 ab
LABSA (µm ²)	522.2 ± 29.7 bc	654.8 ± 100 b	358.8 ± 28 bc	357.7 ± 108.6 bc	490.6 ± 22.1 bc	1138.3 ± 256.6 a	276.8 ± 44.3 c	396.2 ± 103.1 bc
LADSA (µm ²)	427 ± 59.1 a	162.4 ± 35.1 c	136.8 ± 17.4 c	97.2 ± 8.4 c	339.1 ± 39.6 b	155.8 ± 11 c	131.3 ± 16.3 c	99.4 ± 22.4 c

Note: Means sharing same letter with regions are non-significant at $p \leq 0.05$. Abbreviations; LMdTh (midrib thickness), LLmTh (lamina thickness), LABET (abaxial epidermal thickness), LABECA (abaxial epidermal cell area), LADET (adaxial epidermal thickness), LADECA (adaxial epidermal cell area), LABSD (abaxial stomatal density), LADSD (adaxial stomatal density), LABSA (abaxial stomatal area) and LADSA (adaxial stomatal area).

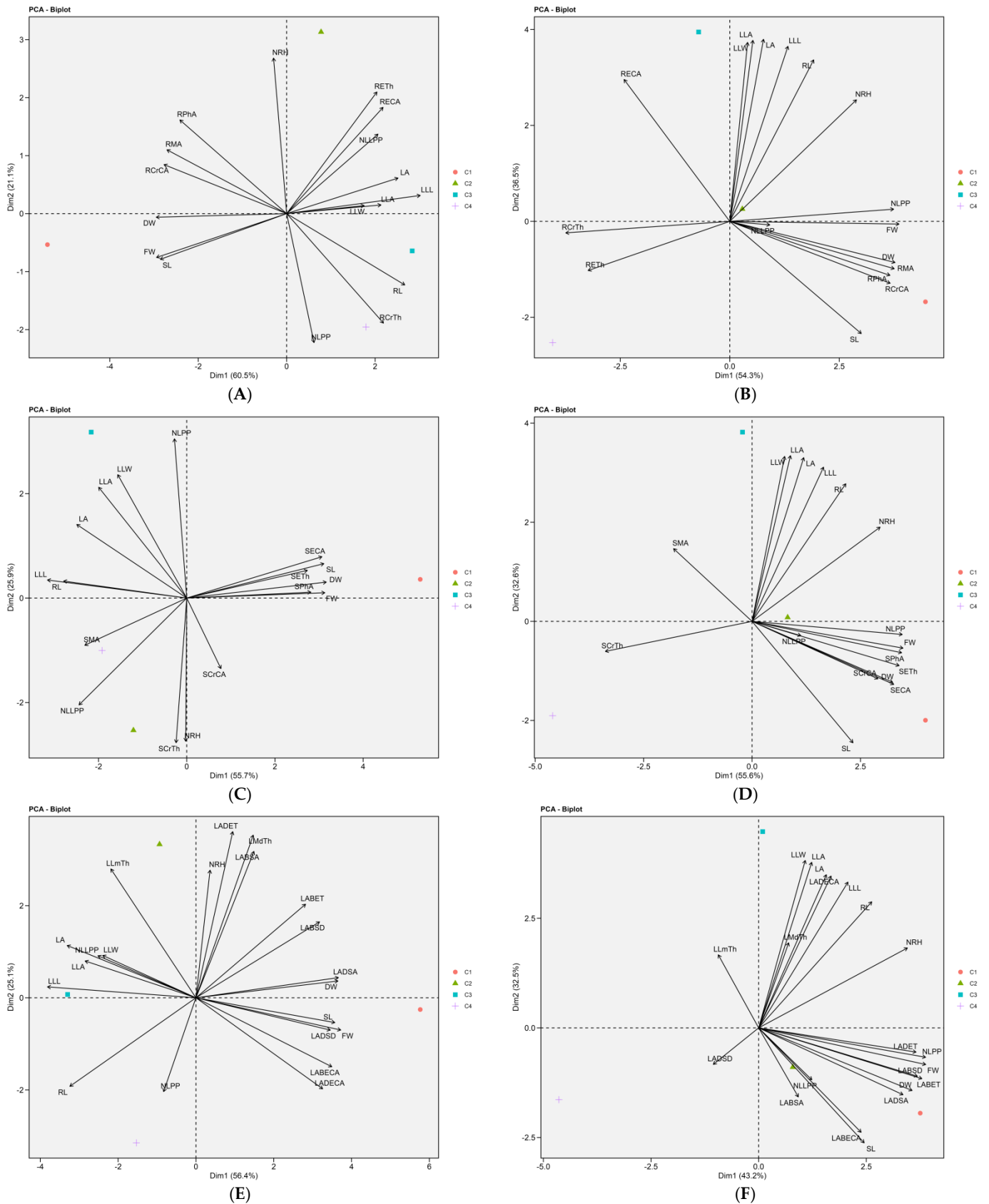


Figure 7. PCA-biplot of morphological traits with (A) root anatomical traits under Pb stress, (B) root anatomical traits under Ni stress, (C) stem anatomical traits under Pb stress, (D) stem anatomical traits under Ni stress, (E) leaf anatomical traits under Pb stress and (F) leaf anatomical traits under Ni stress.

The PCA biplot between morphological and stem anatomical traits showed a total of 81.6% variance (55.7% for PC1 and 25.9% for PC2), with three isolated clusters under Pb stress (Figure 7C). The first cluster showed a strong association among morphological (fresh weight, dry weight and shoot length) and anatomical (epidermal thickness, epidermal cell area and phloem area) traits at 0 mM Pb (C1). The second cluster showed a weak association among morphological traits like number of leaves per plant, leaflet width, leaflet area and leaf area, while there was a strong association among root length and leaflet length at 50 mM Pb (C3). The third cluster showed a strong association between number of root hairs and cortical region thickness at 25 mM Pb (C2) but a weak association with metaxylem area and number of leaflets per plant at 75 mM Pb (C4). Similarly, the PCA biplot between morphological and stem anatomical (under Ni stress) traits showed a total of 88.2% variance (55.6% for PC1 and 32.6% for PC2), with two isolated clusters under Ni stress (Figure 7D). Cluster 1 showed a strong association among morphological traits like leaflet width, leaflet length, leaflet area, leaf area, root length and number of root hairs at 25 mM Ni (C2). The second cluster showed a strong association of number of leaflets per plant, number of leaves per plant, fresh weight and dry weight with phloem area, epidermal thickness, epidermal cell area and cortical cell area at 0 mM Ni (C1).

The PCA biplot between morphological and leaf anatomical traits showed a total of 80.5% variance (56.4% for PC1 and 25.1% for PC2), with four isolated clusters under Pb stress (Figure 7E). Number of root hairs showed a strong association with adaxial epidermal thickness, midrib thickness and abaxial stomatal area, while there was a weak association with abaxial epidermal thickness, abaxial stomatal density and adaxial stomatal density in the first cluster. The second cluster morphological traits (shoot length and fresh weight) showed a strong association with adaxial stomatal density, abaxial epidermal cell area and adaxial epidermal cell area at 0 mM Pb (C1). The third cluster showed a strong association among morphological traits like leaflet width, leaflet length, leaflet area, leaf area and number of leaflets per plant. The fourth cluster showed a weak association between number of leaves per plant and root length at 75 mM Pb (C4). Similarly, the PCA biplot between morphological and leaf anatomical traits showed a total of 75.7% variance (43.2% for PC1 and 32.5% for PC2), with only two isolated groups under Ni stress (Figure 7F). The first cluster showed a strong association among morphological (leaflet width, leaflet length, leaflet area, leaf area, root length and number of root hairs) and anatomical (adaxial epidermal cell area and midrib thickness) traits at 50 mM Ni. The second cluster also showed a strong association among anatomical (adaxial epidermal thickness, abaxial stomatal density, abaxial epidermal thickness, adaxial stomatal area, abaxial epidermal cell area and abaxial stomatal area) and morphological (number of leaves per plant, fresh weight, dry weight and number of leaflets per plant) traits at 0 mM and 25 mM Ni.

3.5. Correlation Analysis

3.5.1. Correlation Analysis between Morphological Traits in Phase 1 and Phase 2

The Pearson correlation analysis showed highly (***) and moderately (** and *) significant positive and negative correlations among morphological traits (in phase 1 under both Pb and Ni stress). Shoot length displayed highly significant positive correlation with number of root hairs, fresh weight, dry weight and number of leaflets per plant, and a moderately negative correlation with leaflets length. The number of root hairs, leaflet area and fresh weight showed highly significant correlations with dry weight, leaf area and dry weight, respectively. The leaflet width had a highly significant correlation with leaf area and leaflet area. The number of leaves per plant also showed a highly significant positive correlation with dry weight, fresh weight and number of leaflets per plant (Figure 8A). Number of root hairs and number of leaves per plant had significant negative correlation with leaflet length. Similarly, in Phase 2 (under both Pb or Ni stress), shoot length had highly significant positive correlation with fresh and dry weight. Root length showed highly significant positive correlation with leaf area and leaflet length and moderately

significant positive correlation with leaflet area and number of leaves per plant. Moreover, number of root hairs, number of leaves per plant, leaflet area and fresh weight displayed highly significant positive correlation with leaflet length, fresh weight, leaf area and dry weight, respectively. Furthermore, leaflet length and leaflet width had highly significant positive correlation with both leaf area and leaflet area (Figure 8B).

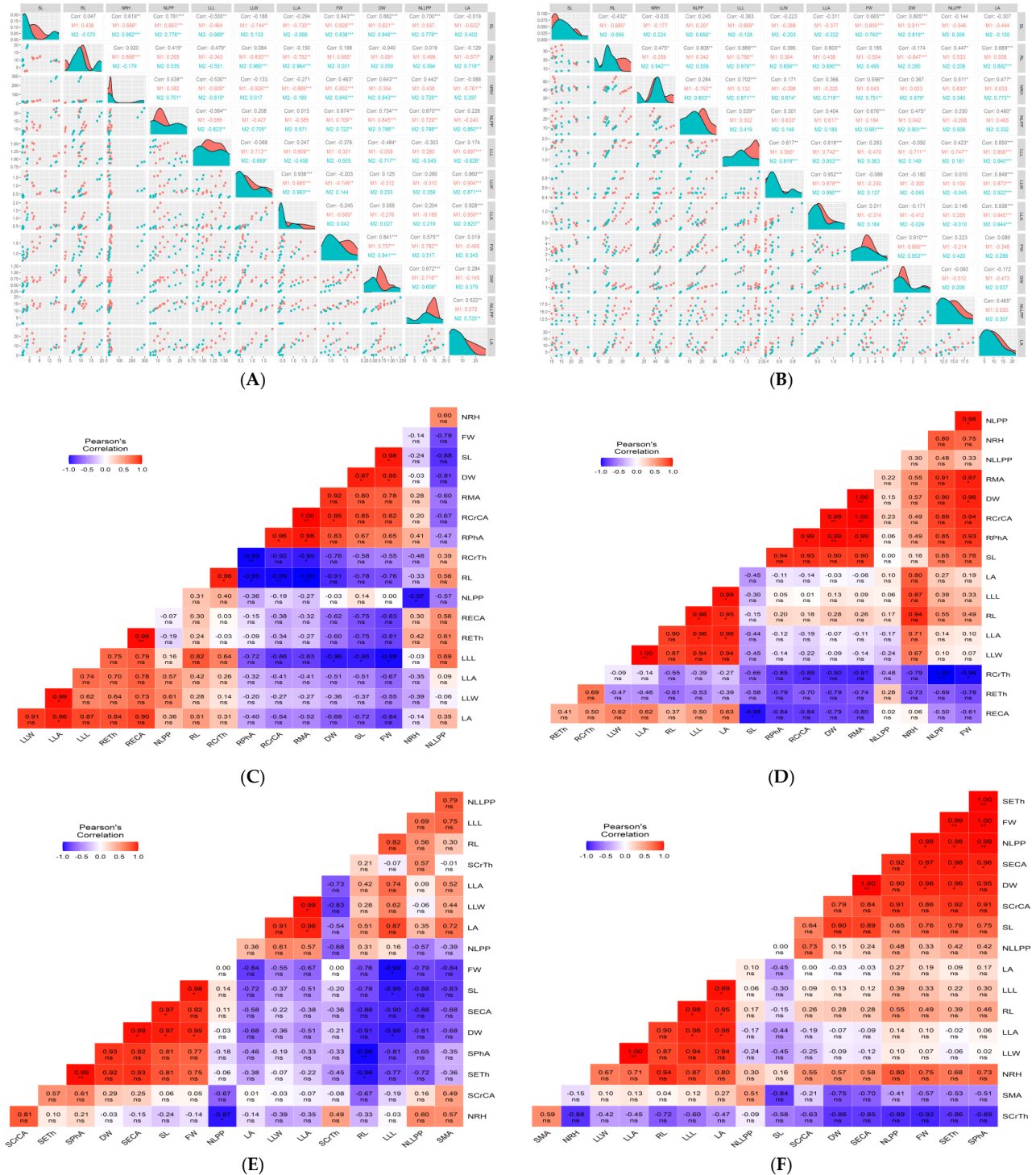


Figure 8. Correlation analysis of morphological traits with (A) morphological traits under Pb stress, (B) morphological traits under Ni stress, (C) root anatomical traits under Pb stress, (D) root anatomical traits under Ni stress, (E) stem anatomical traits under Pb stress and (F) stem anatomical traits under Ni stress. The *, **, and *** indicate significance at $p < 0.05$, $p < 0.01$ and $p < 0.001$, respectively.

and leaflet length with adaxial epidermal cell area. Moreover, the number of leaflets per plant showed highly significant negative correlation with lamina thickness.

3.6. Clustered Heatmaps

Heatmaps were constructed to show bivariate interactions/relationships between morphological and anatomical traits under Pb or Ni stress. Individual cells with different colors indicate the strength of the interaction, and the cells colors are proportional to the strength displayed along the color gradient. The order of rows was determined by hierarchical clustering of rows based on similarity between heavy metal strains under the combined effect of all traits at a given treatment level. A clustered heatmap between morphological and root anatomical traits under Pb stress displayed three main clusters (Figure 10a). Each cluster showed four further subclusters, where leaf area, leaflet width, leaflet area and leaflet length showed a strong relationship with epidermal thickness and cell area. Root length and number of leaves per plant showed a close association with cortical region thickness. In the third sub-cluster, dry weight, shoot length and fresh weight were closely associated with phloem area, cortical cell area and metaxylem area. The number of root hairs and number of leaflets per plant revealed no association with any of the anatomical traits in the fourth sub-cluster. Similarly, a clustered heatmap displayed close association between morphological and root anatomical traits under Ni stress. Morphological traits such as leaflet width, leaflet length, leaflet area, leaf area and root length revealed close associations with each other (Figure 11a). Moreover, dry weight, shoot length and number of leaflets per plant showed close clustering with phloem and cortical cell area.

A clustered heatmap between morphological and stem anatomical traits under Pb stress indicated a close association of shoot length and fresh and dry weight with epidermal thickness, epidermal cell area and phloem area. The number of root hairs was closely associated with cortical cell area, and root length leaflet length and number of leaflets per plant with metaxylem area (Figure 10b). Similarly, a clustered heatmap between morphological and stem anatomical traits under Ni stress displayed a close association of shoot length, fresh weight, dry weight and number of leaves per plant with cortical cell area, epidermal cell area, epidermal thickness and phloem area. Morphological traits such as leaflet width, leaflet length, leaflet area, leaf area, root length and number of root hairs were in close association with each other, while the number of leaflets per plant did not show association with any of the anatomical traits (Figure 11b).

A clustered heatmap between morphological and leaf anatomical traits under Pb stress revealed that shoot length, fresh and dry weight were in close association with adaxial stomatal area, adaxial stomatal density, adaxial epidermal cell area and abaxial epidermal cell area (Figure 10c), while the number of root hairs showed a close association with abaxial stomatal area, abaxial epidermal thickness, adaxial epidermal thickness, abaxial stomatal density and midrib thickness. Moreover, number of leaflets per plant, leaflet length and root did not show any association with anatomical traits. In the fourth cluster, lamina thickness possessed a high similarity with number of leaves per plant, leaflet width, leaflet area and leaf area. A clustered heatmap between morphological and leaf anatomical traits under Ni stress revealed that adaxial epidermal cell area showed a strong association with morphological traits like leaflet width, leaflet length, leaflet area, leaf area and root length (Figure 11c). Shoot length and dry weight showed an association with abaxial epidermal cell area, abaxial stomatal density and adaxial stomatal area. Furthermore, the number of leaflets per plant was associated with adaxial stomatal density and abaxial stomatal area, while the number of root hairs, fresh weight and number of leaves per plant were strongly associated with adaxial and abaxial epidermal thickness.

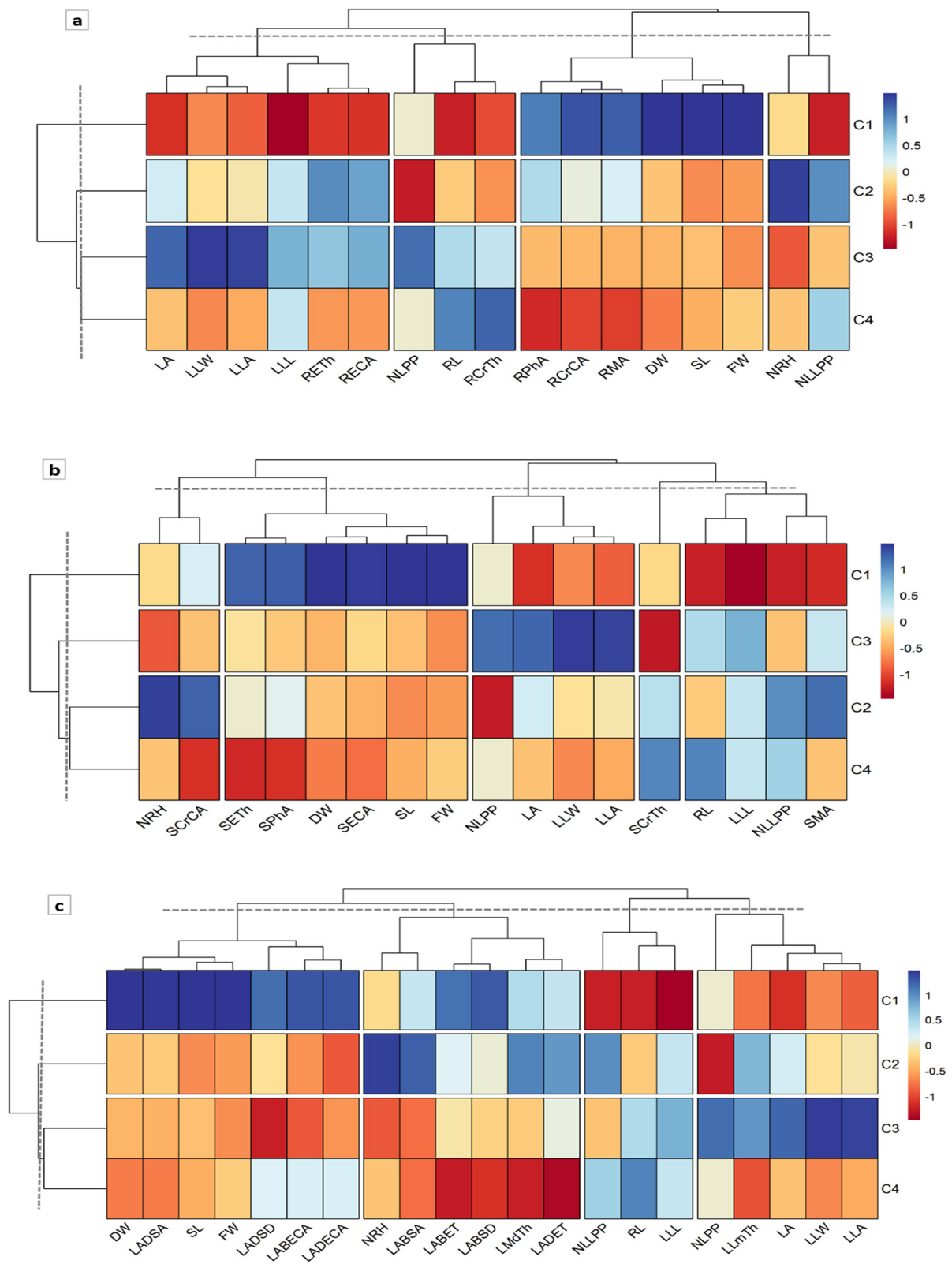


Figure 10. Cluster heatmaps showing grouping of morphological traits with (a) root anatomical, (b) stem anatomical and (c) leaf anatomical traits under Pb stress.

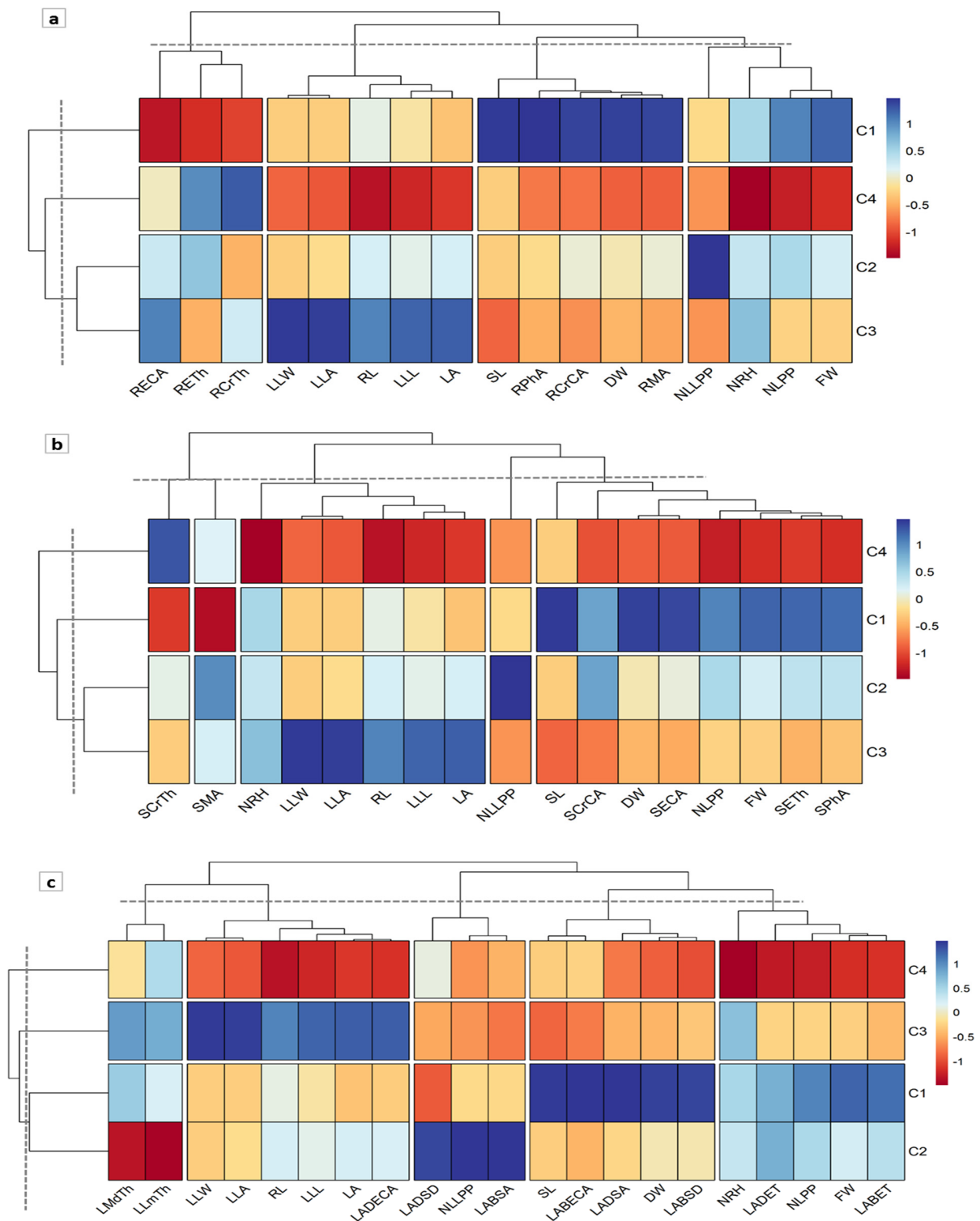


Figure 11. Cluster heatmaps showing grouping of morphological traits with (a) root anatomical, (b) stem anatomical and (c) leaf anatomical traits under Ni stress.

4. Discussion

Understanding plant mechanisms associated with abiotic stress tolerance is challenging due to plants' complex nature and diverse responses. The present investigation focused on evaluating the different morphological and anatomical traits of *A. lebeck* under four different concentrations (0 mM, 25 mM, 50 mM and 75 mM) of Pb or Ni stress, which are ranked among the most toxic heavy metals [52–56]. *A. lebeck* has been found to be an

effective plant species for the removal of heavy metals from soil as a natural source of phytoremediation [57,58]. Plant species have adopted different strategies to cope with Pb or Ni stress by modifying leaf, stem and root anatomical features [59,60]. *A. lebeck* showed different responses to both the heavy metal stress such that growth-related morphological traits were significantly reduced under both Pb and Ni in both phases. Shoot length, fresh weight (g Plant^{-1}), dry weight (g Plant^{-1}), number of root hairs and number of leaves per plant decreased significantly with the increasing concentrations of both Pb and Ni. Additionally leaflet width, leaflet length, and leaflet area increased rather than decreased under both Pb and Ni stress. An exception was noted regarding the consistent increase in root length under both heavy metals stress, which is a feature of tolerance of several plant species to abiotic stresses including heavy metals [61–63]. The root/shoot ratio varies greatly under heavy metals stress among plant species [64–66], and therefore tolerance to heavy metals stress in species like *A. lebeck* can be determined on the basis of root/shoot ratio. Furthermore, plant species like *A. lebeck* with deeper root systems are of great importance because they are capable of extracting heavy metals from polluted soils [67–69]. Both Pb and Ni were more toxic at 75 mM, followed by 50 mM and 25 mM. In comparison with Pb, Ni at 75 mM had more severe effects on plant morphology in the second phase.

The strategic behavior and structural architecture of plant species play important roles in developing tolerance to heavy metals [70]. Structural modifications such as endodermis/epidermis thickness, stomatal orientation and size, sclerification of delicate tissues and storage parenchyma ratio are associated with a degree of stress tolerance in plants [40,71–74]. These modifications are considered indicators of plant survival under heavy metals stress. *A. lebeck* responded differently regarding mechanical, dermal vascular and parenchymatous tissues in root architecture when exposed to both heavy metals stress. Cortical cell area, metaxylem area and phloem area of roots decreased significantly with increasing concentrations of Pb and Ni, while epidermal thickness and cell area increased with increasing concentrations of Pb and Ni. An increase in the epidermal thickness is associated with an increase in the mechanical strength of root tissues. Lysis of cortical parenchyma was observed, along with intensive sclerification in the stelar region. This will reduce tissue damage and, therefore, make possible better survival, even without the function of a major portion of the cortical parenchyma. These results were in agreement with the findings reported by Dos-Reis et al. [75], Guedes et al. [76], Ghafoor et al. [77] and Maia et al. [38]. Furthermore, epidermal thickness, epidermal cell area, phloem area, metaxylem area and cortical region thickness of stem increased with the increase in Pb and Ni concentrations. This is consistent with the results of Al-Saadi et al. [78] in their study on the effects of heavy metals on *Potamogeton*, who also found that anatomical features of plants increased under heavy metal stress.

Leaves are generally more responsive to climatic conditions than any other plant part and therefore modify their anatomical structure according to the type and degree of abiotic stress to develop resistance [61,71]. Anatomical modifications in leaves are strongly associated with heavy metals stress [79], and therefore midrib thickness, abaxial epidermal thickness, adaxial epidermal thickness, abaxial epidermal cell area, abaxial stomatal density and adaxial stomatal density were significantly reduced under stress by both heavy metals. Reduction in leaf anatomical features (especially midrib thickness) is the general impact of heavy metals stress, as reported in several sensitive and tolerant plant species [33,80–82]. Moreover, a reduction in leaf thickness under heavy metals stress is directly associated with low water delivery to the shoot due to inhibiting transpiration via reducing intercellular space, lamina thickness, leaf size and stomatal density [83].

Pearson correlation analysis revealed highly and moderately significant positive and negative correlations among morphological and anatomical traits under both heavy metals stress. Shoot length and root length showed strong and moderate positive correlations with fresh weight, dry weight and leaf morphological traits like leaflet length, width, area and leaf area. Leaflet length and leaflet width showed strong positive correlation with leaflet area, as well as leaf area. Furthermore, root length showed strong negative

correlations with root anatomical features (phloem area, cortical cell area and metaxylem area) stem anatomical features (epidermal thickness and phloem area) and leaf anatomical features (abaxial stomatal density and abaxial epidermal thickness). Fresh weight and number of leaves per plant had strong positive correlation with epidermal thickness, phloem area and abaxial stomatal density but had negative correlations with cortical region thickness. Leaf area, leaflet area and leaflet length showed significant negative correlation with abaxial epidermal cell area and adaxial stomatal density. These correlation analyses confirm the interactions among morphological and anatomical features, which are necessary for developing tolerance to heavy metals stress [44]. These results were in agreement with the earlier finding reported by Akhter et al. [44], Sarwar et al. [61], Guha et al. [84], Papadopoulou et al. [85] and Nakata and Okada [86].

5. Conclusions

In conclusion, both Pb and Ni at different stress levels directly affected the growth and development of *A. lebbbeck* at the seedling stage. Longer exposure (i.e., from phase one to phase two) of *A. lebbbeck* to Pb or Ni stress with high (50 and 75 mM) concentrations led to several modifications at the morphological and anatomical stages. These modifications can help in two ways: (1) improve the understanding of the response of *A. lebbbeck* to Pb or Ni stress, and (2) assist the selection of plants with resistance to these metals for further use in phytoremediation. Moreover, morphological traits like shoot length, fresh and dry weight, number of root hairs, number of leaves per plant and number of leaflets per plant were greatly reduced, while root length, leaflet width, leaflet length and leaflet area increased with the increase in concentration level. An increase in root length indicated that *A. lebbbeck* has the potential to be used to remove Pb and Ni from contaminated soil and can be used as an effective source of phytoremediation. *A. lebbbeck* modified its root, stem and leaf anatomical structures according to the concentration of Pb and Ni. These modifications were helpful in developing tolerance to Pb or Ni stress. For instance, the reduction in leaf thickness prevented water loss by reducing the transpiration rate and maintaining tissue integrity by preventing the collapse of soft parenchyma through intensive lignin deposition in sclerenchymatous tissue. Moreover, positive correlations among morphological and anatomical traits indicated a collective contribution to *A. lebbbeck* survival under heavy metals stress. Overall, both Pb and Ni were more acute at a concentration of 75 mM, followed by 50 mM and 25 mM. We found nickel nitrate to be more toxic to *A. lebbbeck* growth and development than lead nitrate. Furthermore, the underlying genetics behind the modifications in morphological (especially increase in root length) and anatomical traits under Pb or Ni stress should be examined for their relevance to the described findings.

Supplementary Materials: The following supporting information can be downloaded at: <https://www.mdpi.com/article/10.3390/agriculture13071302/s1>, Figure S1: Effect of different Pb and Ni concentrations on anatomical organs (root, stem and leaf) of *A. lebbbeck*; Table S1: Analysis of variance (ANOVA) of morphological and anatomical traits; Table S2: Analysis of Variance (ANOVA) for different anatomical traits of root, stem, and leaf at different levels of Pb and Ni stress.

Author Contributions: Conceptualization, A.B., M.N. and S.R.A.; methodology, M.N., S.R.A., A.B. and S.P.; software and statistical analysis, M.G., A.B., M.N., S.P. and S.R.A.; investigation, M.N., S.R.A., A.B., N.G., Z.K., I.I., S.P. and M.S.T.; data curation, S.R.A., A.B., D.K.Y.T., S.P. and K.R.H.; writing—original draft preparation, M.N., S.R.A., M.G., A.B., I.I., Z.K., S.P., N.G., H.F.A. and M.S.T.; writing—review and editing, M.N., S.R.A., A.B., K.R.H., H.F.A. and D.K.Y.T.; supervision, A.B. All authors have read and agreed to the published version of the manuscript.

Funding: The research work was funded by the Institutional Fund Projects under grant no. (IFPIP: 288-130-1443). The authors gratefully acknowledge technical and financial support provided by the Ministry of Education and King Abdulaziz University, DSR, Jeddah, Saudi Arabia.

Data Availability Statement: Data is contained within the article.

Acknowledgments: The research work was funded by the Institutional Fund Projects under grant no. (IFPIP: 288-130-1443). The authors gratefully acknowledge technical and financial support provided by the Ministry of Education and King Abdulaziz University, DSR, Jeddah, Saudi Arabia.

Conflicts of Interest: The authors declare no conflict of interest.

References

1. UNEP—FAO. *Global Assessment of Soil Pollution—Summary for Policy Makers*; UNEP—FAO: Nairobi, Kenya, 2021.
2. Schmidt-Traub, G.; Kroll, C.; Teksoz, K.; Durand-Delacre, D.; Sachs, J.D. National Baselines for the Sustainable Development Goals Assessed in the SDG Index and Dashboards. *Nat. Geosci.* **2017**, *10*, 547–555. [CrossRef]
3. Rillig, M.C.; Ryo, M.; Lehmann, A.; Aguilar-Trigueros, C.A.; Buchert, S.; Wulf, A.; Iwasaki, A.; Roy, J.; Yang, G. The role of multiple global change factors in driving soil functions and microbial biodiversity. *Science* **2019**, *366*, 886–890. [CrossRef] [PubMed]
4. O’Riordan, R.; Davies, J.; Stevens, C.; Quinton, J.N.; Boyko, C. The ecosystem services of urban soils: A review. *Geoderma* **2021**, *395*, 115076. [CrossRef]
5. Li, G.; Sun, G.X.; Ren, Y.; Luo, X.S.; Zhu, Y.G. Urban soil and human health: A review. *Eur. J. Soil Sci.* **2018**, *69*, 196–215. [CrossRef]
6. Liu, Y.-R.; van der Heijden, M.G.; Riedo, J.; Sanz-Lazaro, C.; Eldridge, D.J.; Bastida, F.; Moreno-Jiménez, E.; Zhou, X.-Q.; Hu, H.-W.; He, J.-Z. Soil contamination in nearby natural areas mirrors that in urban greenspaces worldwide. *Nat. Commun.* **2023**, *14*, 1706. [CrossRef]
7. Zhao, F.-J.; Tang, Z.; Song, J.-J.; Huang, X.-Y.; Wang, P. Toxic metals and metalloids: Uptake, transport, detoxification, phytoremediation, and crop improvement for safer food. *Mol. Plant* **2022**, *15*, 27–44. [CrossRef]
8. Waseem, A.; Arshad, J.; Iqbal, F.; Sajjad, A.; Mehmood, Z.; Murtaza, G. Pollution status of Pakistan: A retrospective review on heavy metal contamination of water, soil, and vegetables. *BioMed Res. Int.* **2014**, *2014*, 813206. [CrossRef]
9. Natasha; Shahid, M.; Khalid, S.; Murtaza, B.; Anwar, H.; Shah, A.H.; Sardar, A.; Shabbir, Z.; Niazi, N.K. A critical analysis of wastewater use in agriculture and associated health risks in Pakistan. *Environ. Geochem. Health* **2020**, 1–20. [CrossRef]
10. Rahman, S.U.; Yasin, G.; Nawaz, M.F.; Cheng, H.; Azhar, M.F.; Riaz, L.; Javed, A.; Li, Y. Evaluation of heavy metal phytoremediation potential of six tree species of Faisalabad city of Pakistan during summer and winter seasons. *J. Environ. Manag.* **2022**, *320*, 115801. [CrossRef]
11. Fahr, M.; Laplaze, L.; Bendaou, N.; Hoher, V.; Mzibri, M.E.; Bogusz, D.; Smouni, A. Effect of lead on root growth. *Front. Plant Sci.* **2013**, *4*, 175. [CrossRef]
12. Tchounwou, P.B. Heavy metal toxicity and the environment, in *Molecular, clinical and environmental toxicology*. *J. Anal. Bioanal. Tech.* **2018**. [CrossRef]
13. Fatemi, H.; Esmail Pour, B.; Rizwan, M. Foliar application of silicon nanoparticles affected the growth, vitamin C, flavonoid, and antioxidant enzyme activities of coriander (*Coriandrum sativum* L.) plants grown in lead (Pb)-spiked soil. *Environ. Sci. Pollut. Res.* **2021**, *28*, 1417–1425. [CrossRef]
14. Fiala, R.; Fialová, I.; Vaculík, M.; Luxová, M. Effect of silicon on the young maize plants exposed to nickel stress. *Plant Physiol. Biochem.* **2021**, *166*, 645–656. [CrossRef] [PubMed]
15. Atta, M.I.; Zehra, S.S.; Dai, D.-Q.; Ali, H.; Naveed, K.; Ali, I.; Sarwar, M.; Ali, B.; Iqbal, R.; Bawazeer, S. Amassing of heavy metals in soils, vegetables and crop plants irrigated with wastewater: Health risk assessment of heavy metals in Dera Ghazi Khan, Punjab, Pakistan. *Front. Plant Sci.* **2022**, *13*, 1080635. [CrossRef] [PubMed]
16. Ashraf, I.; Ahmad, F.; Sharif, A.; Altaf, A.R.; Teng, H. Heavy metals assessment in water, soil, vegetables and their associated health risks via consumption of vegetables, District Kasur, Pakistan. *SN Appl. Sci.* **2021**, *3*, 552. [CrossRef]
17. Ahmad, S.; Khan, M.M.; Rehmani, M.I.A.; Rehmani, M. Heavy Metals Contamination of Soils and Vegetables Irrigated with Municipal Wastewater: A Case Study of Faisalabad. *J. Environ. Agric. Sci.* **2015**, *4*, 2313–8629. Available online: https://www.researchgate.net/publication/277290324_Heavy_Metals_Contamination_of_Soils_and_Vegetables_Irrigated_with_Municipal_Wastewater_A_Case_Study_of_Faisalabad_Pakistan (accessed on 1 May 2023).
18. Manzoor, S.; Shah, M.; Shaheen, N.; Tariq, S.; Khaliq, A.; Jaffar, M. Distribution of Heavy Toxic Metals in Industrial Effluents and Relevant Soils. *J. Chem. Soc. Pak.* **2004**, *26*, 429.
19. Faiz, Y.; Tufail, M.; Javed, M.T.; Chaudhry, M. Road dust pollution of Cd, Cu, Ni, Pb and Zn along islamabad expressway, Pakistan. *Microchem. J.* **2009**, *92*, 186–192. [CrossRef]
20. Abhinaya, M.; Parthiban, R.; Kumar, P.S.; Vo, D.-V.N. A review on cleaner strategies for extraction of chitosan and its application in toxic pollutant removal. *Environ. Res.* **2021**, *196*, 110996. [CrossRef]
21. Pikuła, D.; Stępień, W. Effect of the degree of soil contamination with heavy metals on their mobility in the soil profile in a microplot experiment. *Agronomy* **2021**, *11*, 878. [CrossRef]
22. Zamora-Ledezma, C.; Negrete-Bolagay, D.; Figueroa, F.; Zamora-Ledezma, E.; Ni, M.; Alexis, F.; Guerrero, V.H. Heavy metal water pollution: A fresh look about hazards, novel and conventional remediation methods. *Environ. Technol. Innov.* **2021**, *22*, 101504. [CrossRef]
23. Noor, I.; Sohail, H.; Sun, J.; Nawaz, M.A.; Li, G.; Hasanuzzaman, M.; Liu, J. Heavy metal and metalloid toxicity in horticultural plants: Tolerance mechanism and remediation strategies. *Chemosphere* **2022**, *303*, 135196. [CrossRef] [PubMed]

24. Malik, R.N.; Husain, S.Z.; Nazir, I. Heavy metal contamination and accumulation in soil and wild plant species from industrial area of Islamabad, Pakistan. *Pak. J. Bot.* **2010**, *42*, 291–301.
25. Sarwar, T.; Shahid, M.; Natasha; Khalid, S.; Shah, A.H.; Ahmad, N.; Naeem, M.A.; ul Haq, Z.; Murtaza, B.; Bakhat, H.F. Quantification and risk assessment of heavy metal build-up in soil–plant system after irrigation with untreated city wastewater in Vehari, Pakistan. *Environ. Geochem. Health* **2020**, *42*, 4281–4297. [[CrossRef](#)] [[PubMed](#)]
26. Sajad, M.A.; Khan, M.S.; Bahadur, S.; Shuaib, M.; Naeem, A.; Zaman, W.; Ali, H. Nickel phytoremediation potential of some plant species of the Lower Dir, Khyber Pakhtunkhwa, Pakistan. *Limnol. Rev.* **2020**, *20*, 13–22. [[CrossRef](#)]
27. Jadoon, S.; Muhammad, S.; Hilal, Z.; Ali, M.; Khan, S.; Khattak, N.U. Spatial distribution of potentially toxic elements in urban soils of Abbottabad city, (N Pakistan): Evaluation for potential risk. *Microchem. J.* **2020**, *153*, 104489. [[CrossRef](#)]
28. Murch, S.J.; Haq, K.; Rupasinghe, H.V.; Saxena, P.K. Nickel contamination affects growth and secondary metabolite composition of St. John’s wort (*Hypericum perforatum* L.). *Environ. Exp. Bot.* **2003**, *49*, 251–257. [[CrossRef](#)]
29. Reeves, R.; Baker, A.; Borhidi, A.; Berazain, R. Nickel-accumulating plants from the ancient serpentine soils of Cuba. *New Phytol.* **1996**, *133*, 217–224. [[CrossRef](#)]
30. Liu, W.-C.; Song, R.-F.; Zheng, S.-Q.; Li, T.-T.; Zhang, B.-L.; Gao, X.; Lu, Y.-T. Coordination of plant growth and abiotic stress responses by tryptophan synthase β subunit 1 through modulation of tryptophan and ABA homeostasis in Arabidopsis. *Mol. Plant* **2022**, *15*, 973–990. [[CrossRef](#)]
31. Knudsen, C.; Gallage, N.J.; Hansen, C.C.; Møller, B.L.; Laursen, T. Dynamic metabolic solutions to the sessile life style of plants. *Nat. Prod. Rep.* **2018**, *35*, 1140–1155. [[CrossRef](#)]
32. Pandey, A.K.; Zorić, L.; Sun, T.; Karanović, D.; Fang, P.; Borišev, M.; Wu, X.; Luković, J.; Xu, P. The Anatomical Basis of Heavy Metal Responses in Legumes and Their Impact on Plant–Rhizosphere Interactions. *Plants* **2022**, *11*, 2554. [[CrossRef](#)] [[PubMed](#)]
33. El-Shabasy, A. Effect of heavy metals in the cement dust pollution on morphological and anatomical characteristics of *Cenchrus ciliaris* L. *Saudi J. Biol. Sci.* **2021**, *28*, 1069–1079.
34. El-Okkiah, S.A.; El-Tahan, A.M.; Ibrahim, O.M.; Taha, M.A.; Korany, S.M.; Alsherif, E.A.; AbdElgawad, H.; Sen, E.Z.A.; Sharaf-Eldin, M.A. Under cadmium stress, silicon has a defensive effect on the morphology, physiology, and anatomy of pea (*Pisum sativum* L.) plants. *Front. Plant Sci.* **2022**, *13*, 997475. [[CrossRef](#)]
35. Saraiva, M.P.; Maia, C.F.; da Silva, B.R.S.; Batista, B.L.; Lobato, A.K.d.S. 24-Epibrassinolide induces protection against nickel excess in soybean plants: Anatomical evidences. *Braz. J. Bot.* **2021**, *44*, 197–205. [[CrossRef](#)]
36. Maksimović, I.; Kastori, R.; Krstić, L.; Luković, J. Steady presence of cadmium and nickel affects root anatomy, accumulation and distribution of essential ions in maize seedlings. *Biol. Plant.* **2007**, *51*, 589–592. [[CrossRef](#)]
37. Singh, S.; Srivastava, P.K.; Kumar, D.; Tripathi, D.K.; Chauhan, D.K.; Prasad, S.M. Morpho-anatomical and biochemical adapting strategies of maize (*Zea mays* L.) seedlings against lead and chromium stresses. *Biocatal. Agric. Biotechnol.* **2015**, *4*, 286–295. [[CrossRef](#)]
38. Maia, C.F.; da Silva, B.R.S.; Batista, B.L.; Bajguz, A.; Lobato, A.K.d.S. 24-Epibrassinolide Simultaneously Stimulates Photosynthetic Machinery and Biomass Accumulation in Tomato Plants under Lead Stress: Essential Contributions Connected to the Antioxidant System and Anatomical Structures. *Agronomy* **2022**, *12*, 1985. [[CrossRef](#)]
39. Adejumo, S.A.; Oniosun, B.; Akpoilih, O.A.; Adeseko, A.; Arowo, D.O. Anatomical changes, osmolytes accumulation and distribution in the native plants growing on Pb-contaminated sites. *Environ. Geochem. Health* **2021**, *43*, 1537–1549. [[CrossRef](#)]
40. El-Banna, M.F.; Mosa, A.; Gao, B.; Yin, X.; Wang, H.; Ahmad, Z. Scavenging effect of oxidized biochar against the phytotoxicity of lead ions on hydroponically grown chicory: An anatomical and ultrastructural investigation. *Ecotoxicol. Environ. Saf.* **2019**, *170*, 363–374. [[CrossRef](#)] [[PubMed](#)]
41. Liu, Y.; Wu, Q.; Ge, G.; Han, G.; Jia, Y. Influence of drought stress on alfalfa yields and nutritional composition. *BMC Plant Biol.* **2018**, *18*, 13. [[CrossRef](#)]
42. Mustapha, S.; Shuaib, D.; Ndamitso, M.; Etsuyankpa, M.; Sumaila, A.; Mohammed, U.; Nasirudeen, M. Adsorption isotherm, kinetic and thermodynamic studies for the removal of Pb (II), Cd (II), Zn (II) and Cu (II) ions from aqueous solutions using *Albizia lebbek* pods. *Appl. Water Sci.* **2019**, *9*, 142. [[CrossRef](#)]
43. Yousaf, M.T.B.; Nawaz, M.F.; Khawaja, H.F.; Gul, S.; Ali, S.; Ahmad, I.; Rasul, F.; Rizwan, M. Ecophysiological response of early stage *Albizia lebbek* to cadmium toxicity and biochar addition. *Arab. J. Geosci.* **2019**, *12*, 134. [[CrossRef](#)]
44. Akhter, N.; Aqeel, M.; Hameed, M.; Alhailoul, H.A.S.; Alghanem, S.M.; Shahnaz, M.M.; Hashem, M.; Alamri, S.; Khalid, N.; Al-Zoubi, O.M. Foliar architecture and physio-biochemical plasticity determines survival of *Typha domingensis* pers. Ecotypes in nickel and salt affected soil. *Environ. Pollut.* **2021**, *286*, 117316. [[CrossRef](#)] [[PubMed](#)]
45. Duan, Y.; Zhang, Y.; Zhao, B. Lead, zinc tolerance mechanism and phytoremediation potential of *Alcea rosea* (Linn.) Cavan. and *Hydrangea macrophylla* (Thunb.) Ser. and ethylenediaminetetraacetic acid effect. *Environ. Sci. Pollut. Res.* **2022**, *29*, 41329–41343. [[CrossRef](#)]
46. Pyo, Y.; Kim, G.M.; Choi, S.W.; Song, C.Y.; Yang, S.W.; Jung, I.L. Strontium stress disrupts miRNA biogenesis by reducing HYL1 protein levels in Arabidopsis. *Ecotoxicol. Environ. Saf.* **2020**, *204*, 111056. [[CrossRef](#)]
47. Hermawan, A.A.; Teh, K.L.; Talei, A.; Chua, L.H. Accumulation of heavy metals in stormwater biofiltration systems augmented with zeolite and fly ash. *J. Environ. Manag.* **2021**, *297*, 113298. [[CrossRef](#)] [[PubMed](#)]
48. Shehzad, J.; Mustafa, G.; Arshad, H.; Ali, A.; Naveed, N.H.; Riaz, Z.; Khan, I. Morpho-physiological and biochemical responses of Brassica species toward lead (Pb) stress. *Acta Physiol. Plant.* **2023**, *45*, 8. [[CrossRef](#)]

49. Siddiqui, M.H.; Al-Wahaibi, M.H.; Basalah, M.O. Interactive effect of calcium and gibberellin on nickel tolerance in relation to antioxidant systems in *Triticum aestivum* L. *Protoplasma* **2011**, *248*, 503–511. [[CrossRef](#)]
50. Yang, Y.; Han, X.; Liang, Y.; Ghosh, A.; Chen, J.; Tang, M. The combined effects of arbuscular mycorrhizal fungi (AMF) and lead (Pb) stress on Pb accumulation, plant growth parameters, photosynthesis, and antioxidant enzymes in *Robinia pseudoacacia* L. *PLoS ONE* **2015**, *10*, e0145726. [[CrossRef](#)]
51. Garg, N.; Aggarwal, N. Effect of mycorrhizal inoculations on heavy metal uptake and stress alleviation of *Cajanus cajan* (L.) Millsp. genotypes grown in cadmium and lead contaminated soils. *Plant Growth Regul.* **2012**, *66*, 9–26. [[CrossRef](#)]
52. Han, H.; Cai, H.; Wang, X.; Hu, X.; Chen, Z.; Yao, L. Heavy metal-immobilizing bacteria increase the biomass and reduce the Cd and Pb uptake by pakchoi (*Brassica chinensis* L.) in heavy metal-contaminated soil. *Ecotoxicol. Environ. Saf.* **2020**, *195*, 110375. [[CrossRef](#)] [[PubMed](#)]
53. Altarawneh, R.M. Levels of selected heavy metals (Pb, Ni, Cd, and Cr) in various widely consumed fruits and vegetables in Jordan. *Int. J. Environ. Anal. Chem.* **2021**, *101*, 1026–1033. [[CrossRef](#)]
54. Zhu, Y.; Dong, Y.; Zhu, N.; Jin, H. Foliar application of biosynthetic nano-selenium alleviates the toxicity of Cd, Pb, and Hg in *Brassica chinensis* by inhibiting heavy metal adsorption and improving antioxidant system in plant. *Ecotoxicol. Environ. Saf.* **2022**, *240*, 113681. [[CrossRef](#)]
55. Rahi, A.A.; Younis, U.; Ahmed, N.; Ali, M.A.; Fahad, S.; Sultan, H.; Zarei, T.; Danish, S.; Taban, S.; El Enshasy, H.A. Toxicity of Cadmium and nickel in the context of applied activated carbon biochar for improvement in soil fertility. *Saudi J. Biol. Sci.* **2022**, *29*, 743–750. [[CrossRef](#)]
56. Badawy, I.H.; Hmed, A.A.; Sofy, M.R.; Al-Mokadem, A.Z. Alleviation of cadmium and nickel toxicity and phyto-stimulation of tomato plant l. by endophytic *Micrococcus luteus* and *Enterobacter cloacae*. *Plants* **2022**, *11*, 2018. [[CrossRef](#)]
57. Akintola, O.; Abodunrin, E.; Ademigbuji, A.; Ibode, R.; Babatunde, O. Phytoremediation of potentially toxic elements in waste dumpsite soils by *Albizia lebbek* L. Benth seedlings. *J. For. Res. Manag.* **2022**, *19*, 17–22.
58. Akintola, O.; Ogunbanjo, O.; Adeniran, O.; Abodunrin, E.; Ibode, R. Remediation potential of *Albizia lebbek* L. Benth. in chromium contaminated soil. *J. Res. For. Wildl. Environ.* **2022**, *14*, 95–102.
59. Cai, X.; Jiang, M.; Liao, J.; Yang, Y.; Li, N.; Cheng, Q.; Li, X.; Song, H.; Luo, Z.; Liu, S. Biomass allocation strategies and Pb-enrichment characteristics of six dwarf bamboos under soil Pb stress. *Ecotoxicol. Environ. Saf.* **2021**, *207*, 111500. [[CrossRef](#)] [[PubMed](#)]
60. Ghori, N.-H.; Ghori, T.; Hayat, M.; Imadi, S.; Gul, A.; Altay, V.; Ozturk, M. Heavy metal stress and responses in plants. *Int. J. Environ. Sci. Technol.* **2019**, *16*, 1807–1828. [[CrossRef](#)]
61. Sarwar, Y.; Asghar, A.; Hameed, M.; Fatima, S.; Ahmad, F.; Ahmad, M.S.A.; Ashraf, M.; Shah, S.M.R.; Basharat, S.; Iqbal, U. Structural responses of differentially adapted *Cenchrus setigerus* Vahl ecotypes to water deficit. *Environ. Exp. Bot.* **2022**, *194*, 104746. [[CrossRef](#)]
62. Naz, N.; Rafique, T.; Hameed, M.; Ashraf, M.; Batool, R.; Fatima, S. Morpho-anatomical and physiological attributes for salt tolerance in sewan grass (*Lasiurus scindicus* Henr.) from Cholistan Desert, Pakistan. *Acta Physiol. Plant.* **2014**, *36*, 2959–2974. [[CrossRef](#)]
63. Jing, C.; Cheng, Z.; Li, L.-P.; Sun, Z.-y.; Pan, X.-b. Effects of exogenous salicylic acid on growth and H₂O₂-metabolizing enzymes in rice seedlings under lead stress. *J. Environ. Sci.* **2007**, *19*, 44–49.
64. Sofo, A.; Khan, N.A.; D'Ippolito, I.; Reyes, F. Subtoxic levels of some heavy metals cause differential root-shoot structure, morphology and auxins levels in *Arabidopsis thaliana*. *Plant Physiol. Biochem.* **2022**, *173*, 68–75. [[CrossRef](#)]
65. Abdelmoneim, T.; Moussa, T.; Almaghrabi, O.; Abdelbagi, I. Investigation the effect of arbuscular mycorrhizal fungi on the tolerance of maize plant to heavy metals stress. *Life Sci. J.* **2014**, *11*, 255–263.
66. Ogunkunle, C.O.; Fatoba, P.O.; Awotoye, O.O.; Olorunmaiye, K.S. Root-shoot partitioning of copper, chromium and zinc in *Lycopersicon esculentum* and *Amaranthus hybridus* grown in cement-polluted soil. *Environ. Exp. Biol.* **2013**, *11*, 131–136.
67. Bedair, H.; Ghosh, S.; Abdelsalam, I.M.; Keerio, A.A.; AlKafaas, S.S. Potential implementation of trees to remediate contaminated soil in Egypt. *Environ. Sci. Pollut. Res.* **2022**, *29*, 78132–78151. [[CrossRef](#)]
68. Manikandan, M.; Kannan, V.; Mendoza, O.H.; Kanimozhi, M.; Chun, S.; Pašić, L. The contribution of endophytic bacteria to *Albizia lebbek*-mediated phytoremediation of tannery effluent contaminated soil. *Int. J. Phytoremediation* **2016**, *18*, 77–86. [[CrossRef](#)] [[PubMed](#)]
69. Kabir, M.; Noreen, T.; Iqbal, M.Z.; Shafiq, M.; Athar, M.; Farooqi, Z.-U.-R. The impact of automobile polluted soil on seedling growth performance in some higher plants. *J. Plant Dev.* **2022**, *29*, 103–115. [[CrossRef](#)]
70. Podar, D.; Maathuis, F.J. The role of roots and rhizosphere in providing tolerance to toxic metals and metalloids. *Plant Cell Environ.* **2022**, *45*, 719–736. [[CrossRef](#)]
71. García-Cervigón, A.I.; García-López, M.A.; Pistón, N.; Pugnaire, F.I.; Olano, J.M. Co-ordination between xylem anatomy, plant architecture and leaf functional traits in response to abiotic and biotic drivers in a nurse cushion plant. *Ann. Bot.* **2021**, *127*, 919–929. [[CrossRef](#)]
72. Zanganeh, R.; Jamei, R.; Rahmani, F. Response of maize plant to sodium hydrosulfide pretreatment under lead stress conditions at early stages of growth. *Cereal Res. Commun.* **2021**, *49*, 267–276. [[CrossRef](#)]

73. Maia, C.F.; Pereira, Y.C.; da Silva, B.R.S.; Batista, B.L.; Lobato, A.K.d.S. Exogenously applied 24-epibrassinolide favours stomatal performance, ROS detoxification and nutritional balance, alleviating oxidative damage against the photosynthetic apparatus in tomato leaves under nickel stress. *J. Plant Growth Regul.* **2023**, *42*, 2196–2211. [[CrossRef](#)]
74. Batool, R.; Hameed, M.; Ashraf, M.; Fatima, S.; Nawaz, T.; Ahmad, M.S.A. Structural and functional response to metal toxicity in aquatic *Cyperus alopecuroides* Rottb. *Limnologica* **2014**, *48*, 46–56. [[CrossRef](#)]
75. dos Reis, A.R.; de Queiroz Barcelos, J.P.; de Souza Osório, C.R.W.; Santos, E.F.; Lisboa, L.A.M.; Santini, J.M.K.; dos Santos, M.J.D.; Junior, E.F.; Campos, M.; de Figueiredo, P.A.M. A glimpse into the physiological, biochemical and nutritional status of soybean plants under Ni-stress conditions. *Environ. Exp. Bot.* **2017**, *144*, 76–87. [[CrossRef](#)]
76. Guedes, F.R.C.M.; Maia, C.F.; da Silva, B.R.S.; Batista, B.L.; Alyemini, M.N.; Ahmad, P.; da Silva Lobato, A.K. Exogenous 24-Epibrassinolide stimulates root protection, and leaf antioxidant enzymes in lead stressed rice plants: Central roles to minimize Pb content and oxidative stress. *Environ. Pollut.* **2021**, *280*, 116992. [[CrossRef](#)]
77. Ghafoor, R.; Akram, N.A.; Rashid, M.; Ashraf, M.; Iqbal, M.; Lixin, Z. Exogenously applied proline induced changes in key anatomical features and physio-biochemical attributes in water stressed oat (*Avena sativa* L.) plants. *Physiol. Mol. Biol. Plants* **2019**, *25*, 1121–1135. [[CrossRef](#)]
78. Al-Saadi, S.; Al-Asaadi, W.; Al-Waheeb, A. The effect of some heavy metals accumulation on physiological and anatomical characteristic of some Potamogeton. *L. Plant. J. Ecol. Environ. Sci.* **2013**, *4*, 100–108.
79. Sarath, N.G.; Manzil, S.A.; Ali, S.; Alsahli, A.A.; Puthur, J.T. Physio-anatomical modifications and elemental allocation pattern in *Acanthus ilicifolius* L. subjected to zinc stress. *PLoS ONE* **2022**, *17*, e0263753. [[CrossRef](#)]
80. Fatima, A.; Kataria, S.; Prajapati, R.; Jain, M.; Agrawal, A.K.; Singh, B.; Kashyap, Y.; Tripathi, D.K.; Singh, V.P.; Gadre, R. Magnetopriming effects on arsenic stress-induced morphological and physiological variations in soybean involving synchrotron imaging. *Physiol. Plant.* **2021**, *173*, 88–99. [[CrossRef](#)]
81. Bonanno, G.; Borg, J.A.; Di Martino, V. Levels of heavy metals in wetland and marine vascular plants and their biomonitoring potential: A comparative assessment. *Sci. Total Environ.* **2017**, *576*, 796–806. [[CrossRef](#)]
82. Khosropour, E.; Attarod, P.; Shirvany, A.; Pypker, T.G.; Bayramzadeh, V.; Hakimi, L.; Moeinaddini, M. Response of *Platanus orientalis* leaves to urban pollution by heavy metals. *J. For. Res.* **2019**, *30*, 1437–1445. [[CrossRef](#)]
83. Rucińska-Sobkowiak, R. Water relations in plants subjected to heavy metal stresses. *Acta Physiol. Plant.* **2016**, *38*, 257. [[CrossRef](#)]
84. Guha, A.; Chhajed, S.S.; Choudhary, S.; Sunny, R.; Jansen, S.; Barua, D. Hydraulic anatomy affects genotypic variation in plant water use and shows differential organ specific plasticity to drought in *Sorghum bicolor*. *Environ. Exp. Bot.* **2018**, *156*, 25–37. [[CrossRef](#)]
85. Papadopoulou, S.; Stefi, A.L.; Meletiou-Christou, M.-S.; Christodoulakis, N.S.; Gkikas, D.; Rhizopoulou, S. Structural and Physiological Traits of Compound Leaves of *Ceratonia siliqua* Trees Grown in Urban and Suburban Ambient Conditions. *Plants* **2023**, *12*, 514. [[CrossRef](#)] [[PubMed](#)]
86. Nakata, M.; Okada, K. The leaf adaxial-abaxial boundary and lamina growth. *Plants* **2013**, *2*, 174–202. [[CrossRef](#)] [[PubMed](#)]

Disclaimer/Publisher’s Note: The statements, opinions and data contained in all publications are solely those of the individual author(s) and contributor(s) and not of MDPI and/or the editor(s). MDPI and/or the editor(s) disclaim responsibility for any injury to people or property resulting from any ideas, methods, instructions or products referred to in the content.